Chapter 1

Percolation

1.1 Introduction

Take some squared paper and black out a portion of the squares randomly. Consider the clusters of adjacent black squares. If only a small portion of squares are blacked out, it is unlikely that a cluster extends across opposite sides of the paper. However, if a large portion of squares are blacked out, it is likely that a cluster 'percolates' across the paper. Indeed, for a paper of infinite size, there exists a unique portion of randomly blacked out squares that mark a phase transition from paper with no percolating infinite cluster to paper with a percolating infinite cluster. Percolation is the study of the clusters as a function of the portion of black squares. It is a purely geometrical problem and is arguably the simplest model that undergoes a phase transition. The challenge in percolation lies in describing its emergent structures rather than understanding its defining rules. Apart from investigating the geometrical properties of the percolating infinite cluster, we will be specifically interested in the statistical properties of finite clusters. One approach to studying these clusters is simply to calculate their size and number explicitly from the rules of percolation, but we will find that in general this is a hopeless task even for clusters of moderate size. In the vicinity of the phase transition, another approach to describing cluster statistics suggests itself, and this is related to the notion of scale invariance. We will focus on the phase transition and dwell upon scale invariance, since these are unifying themes throughout the book. We will develop a mathematical framework for expressing scale invariance, applicable not only to percolation, but to other models undergoing a phase transition.

Percolation is, in fact, highly relevant in a variety of physical settings: oil recovery from porous media [King *et al.*, 1999], epidemic modelling [Cardy

and Grassberger, 1985], networks [Cohen *et al.*, 2002], fragmentation [Herrmann and Roux, 1990], metal-insulator transition [Ball *et al.*, 1994], ionic transport in glasses and composites [Roman *et al.*, 1986], fracture patterns and earthquakes in rocks and ground water flow [Sahimi, 1994] among others. Therefore, the concepts in percolation are not only of academic interest but also of considerable practical value. For an introduction to percolation and some of its applications at the level of our presentation, we can recommend the popular text [Stauffer and Aharony, 1994].

After defining percolation and its main observables, our programme is as follows. First, we will investigate one-dimensional percolation, which is simple and exactly solvable. Although trivial, this exercise is not entirely fruitless because it will expose some of the features of a phase transition. Then we will consider percolation on a tree-like lattice where we will also be able to make considerable analytic progress. This so-called mean-field percolation gives a qualitatively more accurate description of a phase transition, but leaves out important features, both qualitative and quantitative, that are present in percolation in general. In two dimensions, we will initially appear to reach an impasse, since the possibility that clusters 'interact' with themselves will force us to abandon explicit calculations even for clusters of moderate size. Fortunately, however, one-dimensional and mean-field percolation provide clues suggesting that something generic happens to the clusters near a phase transition. We will identify and exploit this generic phenomenon by invoking the powerful concept of scale invariance. This will allow us to propose a particular functional form for the statistics of clusters. While this so-called scaling ansatz will not be able to give us the exact statistics of clusters, we will argue that the concept of scale invariance nonetheless gives us something far more preferable: a statistical framework for unifying the description of clusters in percolation in general.

When studying the geometrical properties of percolation in greater detail, we will find that the root of the simplification of scale invariance lies in the fractal nature of percolation at a phase transition. Loosely speaking, this means that at a phase transition percolating systems look alike on different scales. This in turn will refine our intuition of scale invariance, and we will be in a position to introduce the so-called renormalisation group approach. Such an approach is designed to exploit scale invariance in percolation at the phase transition, by preserving only large-scale features of the clusters. We will illustrate this approach with specific examples of renormalisation group transformations.

1.1.1 *Definition of site percolation*

We now define site percolation, one of the simplest examples of a disordered system. Consider for now a two-dimensional square lattice composed of $L \times L$ sites. We refer to L, measured in units of the lattice spacing, as the lattice size. Note that L is not a length scale as such, but a dimensionless number, L'/a, where L' is the lattice length and a the lattice spacing. Throughout, all lengths are measured in units of the lattice spacing.

To introduce disorder, we occupy sites randomly and independently with occupation probability p, treating all sites equally, see Figure 1.1. The foremost entity of interest is a cluster, which we define as a group of nearest-neighbouring occupied sites. The cluster size, s, is the number of occupied sites in the group.

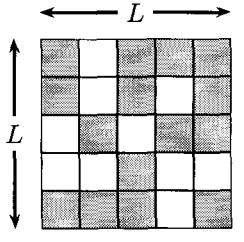

s	$N(s,p;L)$
1	2
2	1
4	1
7	1

Fig. 1.1 A realisation of two-dimensional site percolation on a square lattice of size $L = 5$. Sites are occupied with probability p and are thus empty with probability $(1 - p)$. Occupied sites are dark grey while unoccupied sites are white. A cluster is defined as a group of nearest-neighbouring occupied sites. In a square lattice, a bulk site has four nearest neighbours: north, south, east, and west and four next-nearest-neighbours: north-east, north-west, south-east, and south-west. The table to the right displays the cluster size frequency, $N(s,p;L)$.

1.1.2 *Quantities of interest*

We shall introduce the quantities of interest on a two-dimensional square lattice. For a fixed lattice size L measured in units of the lattice spacing, there is only one parameter in the problem, namely the occupation probability p.

For $p = 0$ the lattice is empty of clusters, while for $p = 1$ there is only one cluster of size L^2. For intermediate values $0 < p < 1$, each realisation will, in general, be different. But qualitatively, we expect the size of the largest cluster to increase with p. Figure 1.2 supports this trend, showing six realisations of increasing p on a lattice of size $L = 150$.

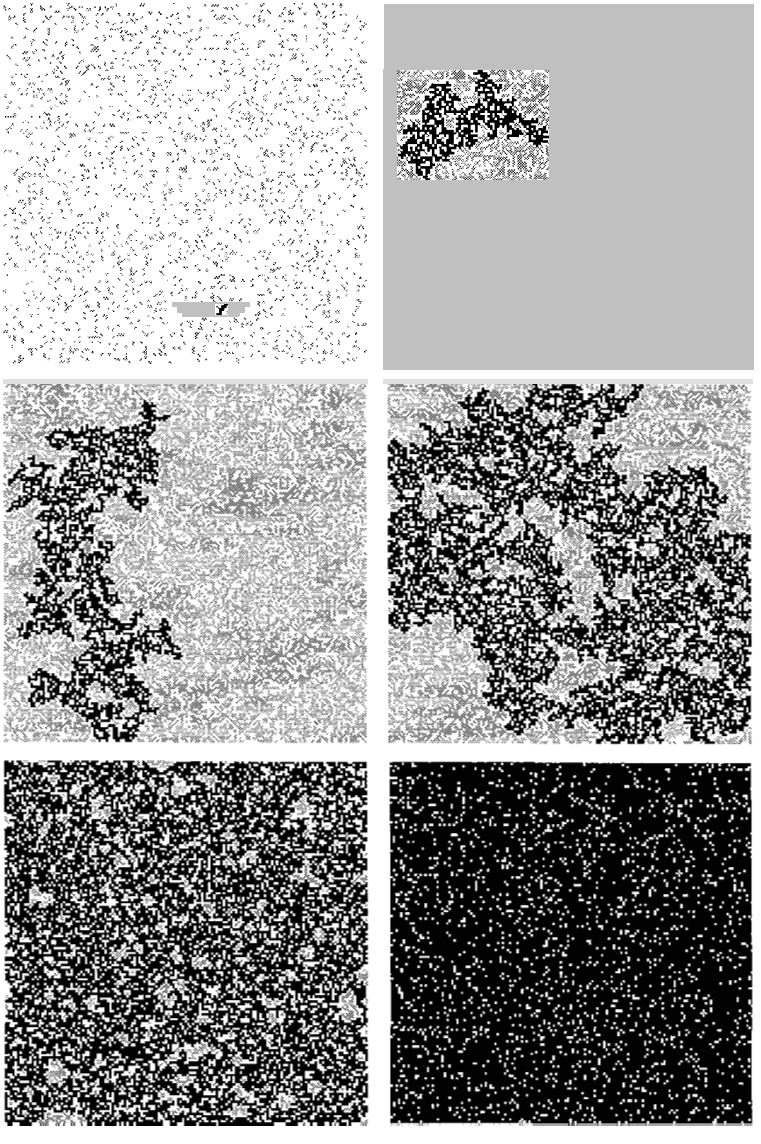

Fig. 1.2 Six realisations of two-dimensional site percolation on a square lattice of size $L = 150$ for occupation probabilities $p = 0.10, 0.55, 0.58, 0.59274621, 0.65, 0.90$, from left to right and top to bottom, respectively. Occupied sites are dark grey while unoccupied sites are white. For each realisation, the largest cluster has been shaded black.

For each realisation, the largest cluster has been shaded black. In fact, for a given p, there is a whole distribution of cluster sizes. It is one of our main aims to determine this distribution, since we would be able to calculate the probability of clusters of any size, including the average cluster size, for example.

By definition, a cluster is percolating if and only if it is infinite. Clearly, clusters that span a finite lattice from left to right or top to bottom are candidates for percolating clusters in infinite systems. In Figure 1.2, for example, the largest clusters in the lattices corresponding to $p = 0.59274621, 0.65$, and 0.90 are spanning clusters whereas the largest clusters in the lattices corresponding to $p = 0.10, 0.55$ and 0.58 are not. The largest cluster in the lattice corresponding to $p = 0.58$, however, is almost spanning.

In an infinite system, there exists a critical occupation probability, p_c, such that for $p < p_c$ there is no percolating infinite cluster, while for $p > p_c$ there is a percolating infinite cluster. At $p = p_c$, it has been conjectured and shown rigorously for $d = 2$, that there is no percolating infinite cluster [Grimmett, 1999]. The large but finite clusters that emerge at $p = p_c$ are called 'incipient infinite clusters'. Throughout, we will often refer to the incipient infinite clusters at $p = p_c$ as percolating clusters, even though they are, strictly speaking, finite.

In an infinite system, how much space does the percolating cluster occupy of the lattice or, in other words, what is the probability that a site belongs to the percolating cluster? What type of geometry does the percolating cluster exhibit? For example, is it fractal? Excluding the percolating infinite cluster, what is the typical 'radius' of the largest finite cluster? As a closely related question, what is the probability that two sites belong to the same finite cluster? Similarly, excluding the percolating infinite cluster, what is the typical 'size' of the largest finite cluster? How is the typical size of the largest finite cluster related with its typical radius? These are some of the questions we will now try to answer.

1.2 Percolation in $d = 1$

We start with one-dimensional percolation, because this is one of the few cases where we are able to calculate quantities exactly. Although the conclusions we reach in one dimension are not general to higher dimensions, some of the main features of percolation are nevertheless present.

1.2.1 *Cluster number density*

Figure 1.3 is a realisation of site percolation in a one-dimensional lattice of size $L = 20$ where sites are occupied with probability p.

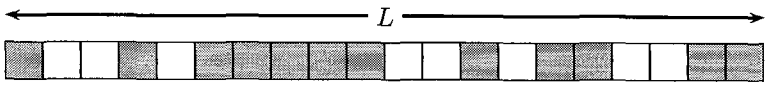

Fig. 1.3 A realisation of one-dimensional site percolation on a lattice of size $L = 20$. Occupied sites are dark grey while unoccupied sites are white. There are three clusters of size $s = 1$, two clusters of size $s = 2$, and one cluster of size $s = 5$.

We can readily construct the cluster size frequency, $N(s, p; L)$. There are three clusters of size $s = 1$, two clusters of size $s = 2$, and one cluster of size $s = 5$. This cluster size frequency pertains to a particular realisation on a given lattice of size L, but we would like to be far more general. We therefore proceed by accounting for the lattice size and calculating cluster size frequencies probabilistically. In doing so, we encounter our first complication with L being finite. This is because the two boundary sites have only one nearest neighbour each, while bulk sites have two nearest neighbours each. For example, consider the cluster of size $s = 5$ in Figure 1.3. If the cluster is in the bulk of the lattice, five consecutive sites would be occupied, while the two sites on either side of the cluster would be unoccupied. If the cluster touches the boundary of the lattice, there would still be five consecutive sites occupied, but only one site unoccupied. However, the ratio of boundary to bulk sites tends to zero for hypercubic lattices as L tends to infinity. Therefore, such a complication would play a diminishing role with increasing L, and completely disappears for an infinite system. From now on, we will therefore ignore the effect of boundary sites.

We are now ready to calculate the probability that a given site belongs to a cluster of size s. The site must be part of a consecutive group of s occupied sites bounded by two unoccupied sites. The probability for this is $s(1-p)p^s(1-p)$, where the factor s comes about because the given site can be any of the s occupied sites. This expression is a simple product because each site is occupied independently with probability p and therefore unoccupied with probability $(1-p)$.

How is this quantity related to the cluster size frequency $N(s, p; L)$? Since $s(1-p)^2p^s$ is the probability that a given site belongs to a cluster of size s, we might try to identify $Ls(1-p)^2p^s$ with $N(s, p; L)$. But this reasoning would be wrong, because an s-cluster takes up s sites, so there

is only space for approximately L/s such clusters. Therefore, to calculate the expected frequency of s-clusters in a lattice of size L, we must correct our estimate by dividing by s, that is,

$$N(s,p;L) = L(1-p)^2 p^s. \tag{1.1}$$

The cluster number frequency, however, is not a desirable quantity, because it depends on the lattice size L. Therefore, we normalise by the number of sites in the lattice, and work instead with the cluster number density,

$$n(s,p) = \frac{N(s,p;L)}{L} = (1-p)^2 p^s. \tag{1.2}$$

In this notation, $sn(s,p)$ is the probability that a given site belongs to an s-cluster. Figure 1.4 displays $n(s,p)$ versus cluster size s for five different probabilities p.

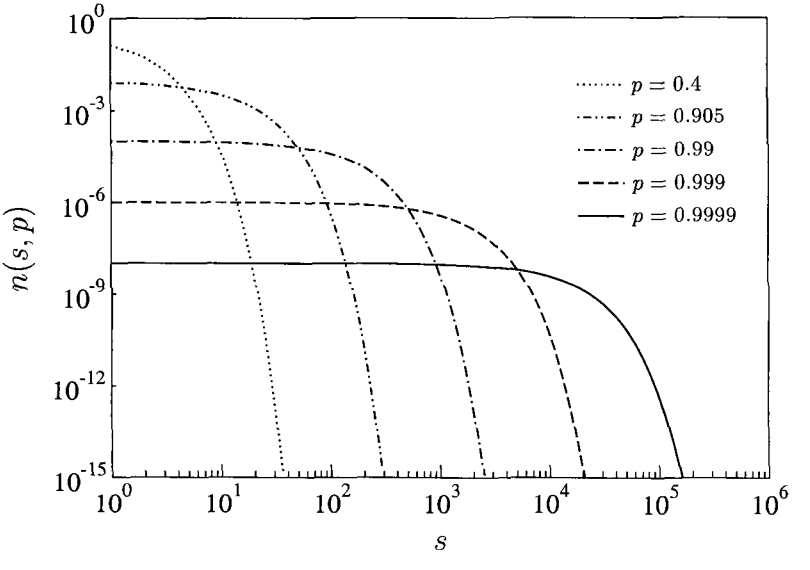

Fig. 1.4 Exact solution of the cluster number density, $n(s,p)$, versus the cluster size, s, for one-dimensional percolation. The five curves correspond to occupation probabilities $p = 0.4, 0.905, 0.99, 0.999, 0.9999$ with characteristic cluster sizes $s_\xi(p) \approx 1, 10, 100, 1\,000, 10\,000$, respectively. For $p \to 1^-$, the characteristic cluster size diverges.

For a given p, the cluster number density $n(s,p)$ decreases with increasing cluster size s, thus large clusters are rare. For large p, the curve remains relatively flat for a large range of s, before decaying rapidly. This motivates

the introduction of a 'characteristic' cluster size, $s_\xi(p)$, signalling the onset of the rapid decay. A commonly accepted convention is to mark where the curve has decreased by a factor $1/e$, see Figure 1.4. We can recast the cluster number density in a form revealing this behaviour:

$$\begin{aligned} n(s,p) &= (1-p)^2 p^s \\ &= (1-p)^2 \exp\left(\ln p^s\right) \\ &= (1-p)^2 \exp\left(s \ln p\right) \\ &= (1-p)^2 \exp\left(-s/s_\xi\right), \end{aligned} \tag{1.3}$$

with the definition of the characteristic cluster size

$$s_\xi(p) = -\frac{1}{\ln p}, \tag{1.4}$$

which is a function of p, plotted in Figure 1.5(a). The characteristic cluster size is an increasing function of p and diverges when p tends to one from below. To investigate how $s_\xi(p)$ diverges as p approaches one, we use the Taylor expansion $\ln(1-x) \to -x$ for $x \to 0$, see Appendix A, for the denominator in the neighbourhood of $p = 1$ to find

$$s_\xi(p) = -\frac{1}{\ln\left(1-[1-p]\right)} \to (1-p)^{-1} \quad \text{for } p \to 1^-. \tag{1.5}$$

Thus, the characteristic cluster size diverges as a power law with exponent -1 in terms of $(1-p)$, the distance of p below one, see Figure 1.5(b).

1.2.2 *Average cluster size*

What is the average cluster size? For example, in Figure 1.3 there are three clusters of size one, two clusters of size two, and one cluster of size five. Therefore, the average size of the $N_{\text{clu}} = 6$ clusters is

$$\frac{1}{N_{\text{clu}}} \sum_{k=1}^{N_{\text{clu}}} s_k = \frac{1+1+1+2+2+5}{6} = 2. \tag{1.6}$$

Here, each cluster has equal weight. However, there is an alternative form of averaging where each cluster is weighted according to its size, giving more weight to large clusters. To understand this type of averaging, imagine choosing an occupied site at random. How large, on average, is the cluster to which this occupied site belongs? In our example, there are twelve occupied sites. The probability of choosing a particular occupied site is $1/N_{\text{occ}}$, where $N_{\text{occ}} = 12$ is the total number of occupied sites. The probability that the

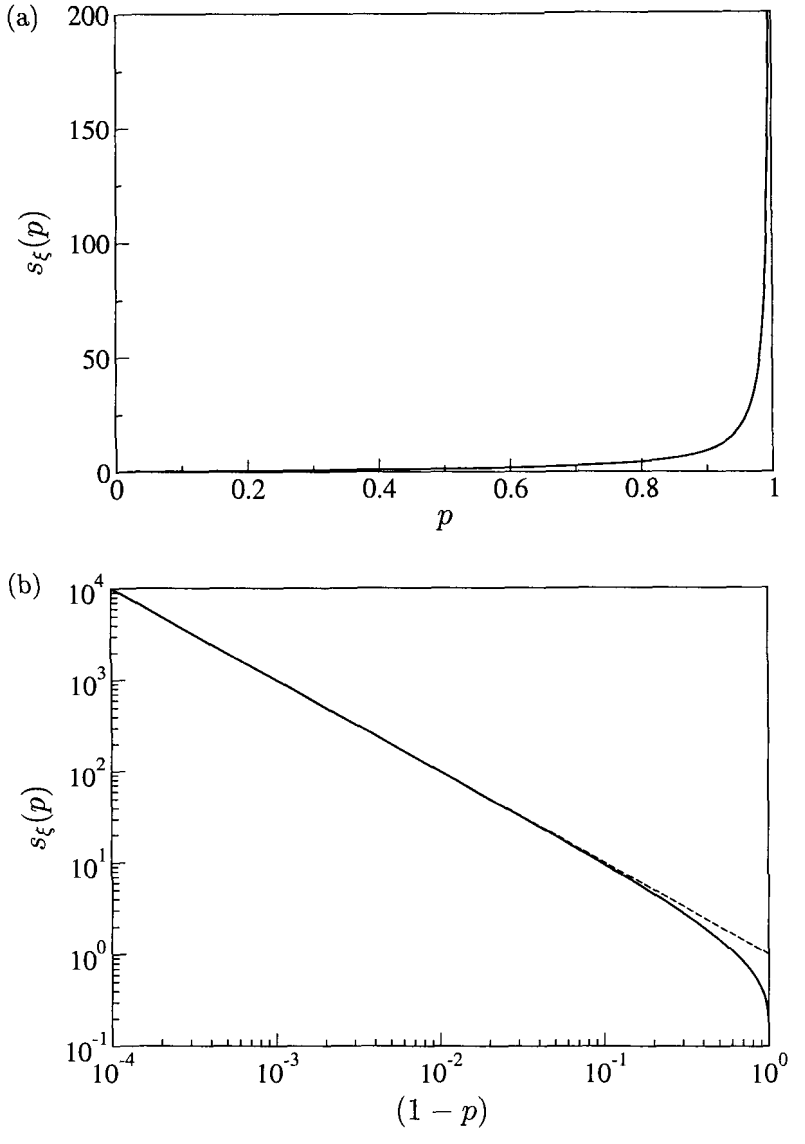

Fig. 1.5 Exact solution of the characteristic cluster size for one-dimensional percolation. (a) The characteristic cluster size, $s_\xi(p)$, versus the occupation probability, p. For p approaching one, the characteristic cluster size diverges. For p tending to zero, $s_\xi(p)$ tends to zero. (b) The characteristic cluster size, $s_\xi(p)$, versus $(1-p)$, the distance of p below one (solid line). For $p \to 1^-$, the characteristic cluster size diverges as a power law with exponent -1 in terms of $(1-p)$. The dashed straight line has slope -1.

chosen site belongs to a particular s-cluster is s/N_{occ}. Weighting each of the N_{clu} clusters by its size, the average size of a cluster to which a randomly chosen occupied site belongs is

$$\chi(p) = \frac{1}{N_{\text{occ}}} \sum_{k=1}^{N_{\text{clu}}} s_k^2 = \frac{1^2 + 1^2 + 1^2 + 2^2 + 2^2 + 5^2}{12} = 3. \tag{1.7}$$

From now on, we will take the average cluster size to be $\chi(p)$. We would like to relate $\chi(p)$ to the cluster number density $n(s,p)$. First we convert the sum running over all clusters indexed by k, to a sum running over all cluster sizes s. This is achieved by replacing a sample of clusters with their frequency,

$$\chi(p) = \frac{1}{N_{\text{occ}}} \sum_{k=1}^{N_{\text{clu}}} s_k^2 = \frac{1}{N_{\text{occ}}} \sum_{s=1}^{\infty} s^2 N(s,p;L). \tag{1.8}$$

In a lattice of size L, the expected number of occupied sites, $N_{\text{occ}} = pL$, and therefore

$$\begin{aligned} \chi(p) &= \frac{\sum_{s=1}^{\infty} s^2 N(s,p;L)}{pL} \\ &= \frac{\sum_{s=1}^{\infty} s^2 n(s,p)}{p} \\ &= \frac{\sum_{s=1}^{\infty} s^2 n(s,p)}{\sum_{s=1}^{\infty} s n(s,p)} \quad \text{for } p < 1. \end{aligned} \tag{1.9}$$

To justify the last step in Equation (1.9), we point out that the probability that an arbitrary site in the lattice belongs to any finite cluster is simply the probability p of it being occupied. This is true for all $p < 1$. The probability that an arbitrary site belongs to an s-cluster is given by $sn(s,p)$. Therefore, the sum of $sn(s,p)$ over all possible s-clusters equals p, the probability that a site is occupied, and we have the sum rule

$$\sum_{s=1}^{\infty} s n(s,p) = p \quad \text{for } p < 1. \tag{1.10}$$

Notice that at $p = 1$, the above identity breaks down: according to Equation (1.2), $n(s,1) = 0$, making the left-hand side of Equation (1.10) equal to zero, while the right hand-side equals one. The inconsistency occurs because, at $p = 1$, there is only one cluster present and it is infinite in size. We can demonstrate the identity in Equation (1.10) for $p < 1$ rigorously by

summing up a geometric series, that is,

$$\begin{aligned}\sum_{s=1}^{\infty} sn(s,p) &= \sum_{s=1}^{\infty} s(1-p)^2 p^s \\ &= (1-p)^2 \sum_{s=1}^{\infty} p\frac{d}{dp}p^s \\ &= (1-p)^2 \left(p\frac{d}{dp}\right)\left(\sum_{s=1}^{\infty} p^s\right) \\ &= (1-p)^2 \left(p\frac{d}{dp}\right)\left(\frac{p}{1-p}\right) \\ &= p. \end{aligned} \tag{1.11}$$

We will take the latter form in Equation (1.9) as the definition of the average cluster size $\chi(p)$, also in dimensions $d > 1$ [Stauffer and Aharony, 1994]. The average cluster size is therefore

$$\begin{aligned}\chi(p) &= \frac{\sum_{s=1}^{\infty} s^2 n(s,p)}{\sum_{s=1}^{\infty} sn(s,p)} \\ &= \frac{1}{p}(1-p)^2 \sum_{s=1}^{\infty} s^2 p^s \\ &= \frac{1}{p}(1-p)^2 \left(p\frac{d}{dp}\right)\left(p\frac{d}{dp}\right)\left(\sum_{s=1}^{\infty} p^s\right). \end{aligned} \tag{1.12}$$

After cautioning the reader that

$$\left(p\frac{d}{dp}\right)\left(p\frac{d}{dp}\right) \neq p^2\frac{d^2}{dp^2}, \tag{1.13}$$

we finally arrive at

$$\chi(p) = \frac{1+p}{1-p} \quad \text{for } 0 < p < 1. \tag{1.14}$$

As expected, the average cluster size is an increasing function of p, see Figure 1.6(a). Like the characteristic cluster size, when p approaches one, the average cluster size also diverges as a power law with exponent -1 in terms of $(1-p)$, the distance of p below one,

$$\chi(p) = \frac{1+p}{1-p} \to 2(1-p)^{-1} \quad \text{for } p \to 1^-, \tag{1.15}$$

see Figure 1.6(b).

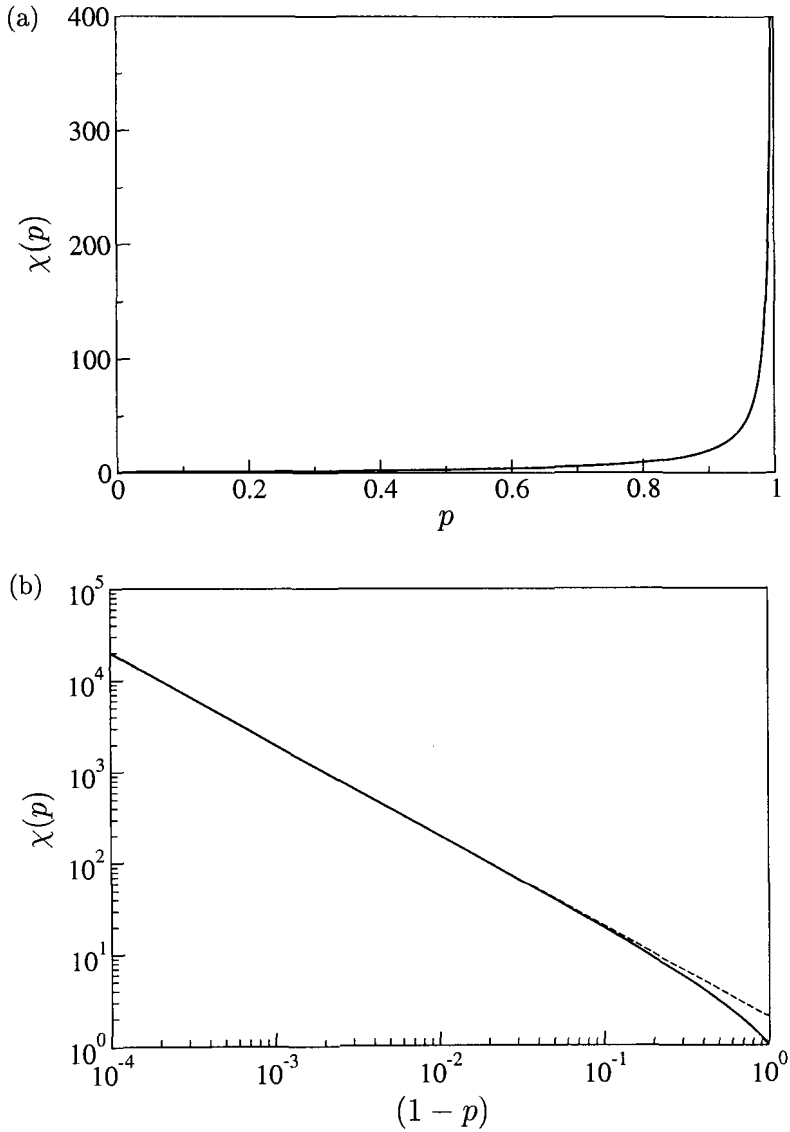

Fig. 1.6 Exact solution of the average cluster size for one-dimensional percolation. (a) The average cluster size, $\chi(p)$, versus the occupation probability, p. For p approaching one, the average cluster size diverges. For p tending to zero, $\chi(p)$ tends to one. (b) The average cluster size, $\chi(p)$, versus $(1-p)$, the distance of p below one (solid line). For $p \to 1^-$, the average cluster size diverges as a power law with exponent -1 in terms of $(1-p)$. The dashed straight line has slope -1.

1.2.3 *Transition to percolation*

The probability that a site belongs to any finite cluster is p. In one dimension, the percolating infinite cluster must include every site in the lattice for it to span from left to right. What is the probability, $P_\infty(p)$, that a site belongs to the percolating cluster? For $p < 1$, there is no percolating cluster, so the probability that a site belongs to the percolating cluster is zero. However, at $p = 1$, there is a percolating cluster and all sites belong to it. Thus the probability that a site belongs to the percolating cluster is one, that is,

$$P_\infty(p) = \begin{cases} 0 & \text{for } p < 1 \\ 1 & \text{for } p = 1. \end{cases} \tag{1.16}$$

This quantity allows us to generalise Equation (1.10) to

$$P_\infty(p) + \sum_{s=1}^{\infty} sn(s,p) = p \tag{1.17}$$

valid for all p. Put differently, Equation (1.17) states that the probability that a site is occupied, p, is equal to the probability that the site belongs to the percolating infinite cluster, $P_\infty(p)$, added to the probability that the site belongs to a finite cluster, $\sum_{s=1}^{\infty} sn(s,p)$. In fact, Equation (1.17) is valid in higher dimensions as well.

1.2.4 *Correlation function*

The final quantity to be discussed in one dimension is the probability that two sites belong to the same finite cluster. More precisely, let $\mathbf{r}_i$ denote the position vector of site i in the one-dimensional lattice. Given that the site at $\mathbf{r}_i$ is occupied, the probability that a site at position $\mathbf{r}_j$ belongs to the same finite cluster is known as the site-site correlation function. Since the site at position $\mathbf{r}_j$ must be occupied as well as all the $r - 1$ intermediate sites, the site-site correlation function

$$g(\mathbf{r}_i, \mathbf{r}_j) = p^r \quad \text{for } 0 < p < 1, \tag{1.18}$$

where $r = |\mathbf{r}_i - \mathbf{r}_j|$ is the distance between the sites measured in units of the lattice spacing. By definition, $g(\mathbf{r}_i, \mathbf{r}_i) = 1$ when $r = 0$. The correlation function decays with increasing distance r. In the same spirit as for the characteristic cluster size $s_\xi(p)$, we can characterise the decay of the site-site

correlation function,

$$g(\mathbf{r}_i, \mathbf{r}_j) = \exp(\ln p^r) = \exp(r \ln p) = \exp(-r/\xi), \tag{1.19}$$

where we have defined a characteristic length scale, $\xi(p)$, the correlation length (measured in units of the lattice spacing) by

$$\xi(p) = -\frac{1}{\ln p} = -\frac{1}{\ln(1-[1-p])} \to (1-p)^{-1} \quad \text{for } p \to 1^-. \tag{1.20}$$

Again we have used the Taylor expansion $\ln(1-x) \to -x$ for $x \to 0$, see Appendix A. The correlation length diverges as a power law with exponent -1 in terms of $(1-p)$, the distance of p below one. Note that the correlation length is the typical radius of the largest cluster. For this reason we have used the notation $s_\xi(p)$ to denote the characteristic cluster size.

In fact, the correlation function $g(\mathbf{r}_i, \mathbf{r}_j)$ is related to the average cluster size $\chi(p)$. Consider an occupied site at position $\mathbf{r}_i$. The probability that a site at position $\mathbf{r}_j$ is occupied and belongs to the same cluster is $g(\mathbf{r}_i, \mathbf{r}_j)$, hence

$$\begin{aligned}
\sum_{\mathbf{r}_j} g(\mathbf{r}_i, \mathbf{r}_j) &= \sum_{\mathbf{r}_j} p^{|\mathbf{r}_i - \mathbf{r}_j|} \\
&= \cdots + p^2 + p^1 + p^0 + p^1 + p^2 + \cdots \\
&= \frac{1+p}{1-p} \\
&= \chi(p),
\end{aligned} \tag{1.21}$$

which the reader can show by summing the geometric series.

1.2.5 *Critical occupation probability*

We conclude our analysis of one-dimensional percolation by remarking on the role played by the occupation probability $p = 1$. Approaching this value, the characteristic cluster size $s_\xi(p)$, the average cluster size $\chi(p)$, and the correlation length $\xi(p)$, all diverge. This is intimately related to the onset of percolation at $p = 1$. To mark the transition to a percolating phase, the probability $p = 1$ is referred to as the critical occupation probability, p_c. The divergence of the above characteristic quantities may be expressed as a power law in terms of $(p_c - p)$, the distance of p below p_c.

1.3 Percolation on the Bethe Lattice

In one-dimensional percolation, it is not hard to calculate the cluster number density $n(s,p)$, thereby obtaining various quantities of interest such as the characteristic cluster size $s_\xi(p)$ and the average cluster size $\chi(p)$, as well as determining the critical occupation probability p_c. In the Bethe lattice, a mathematical construct also known as the Cayley tree, it is also possible to obtain analytical results for the above quantities [Fisher and Essam, 1961]. As we shall see, one-dimensional and Bethe lattices share the simplifying property of having no loops: any two sites in such lattices have a unique path between them.

1.3.1 *Definition of the Bethe lattice*

A Bethe lattice is a tree where each site has z neighbours, see Figure 1.7.

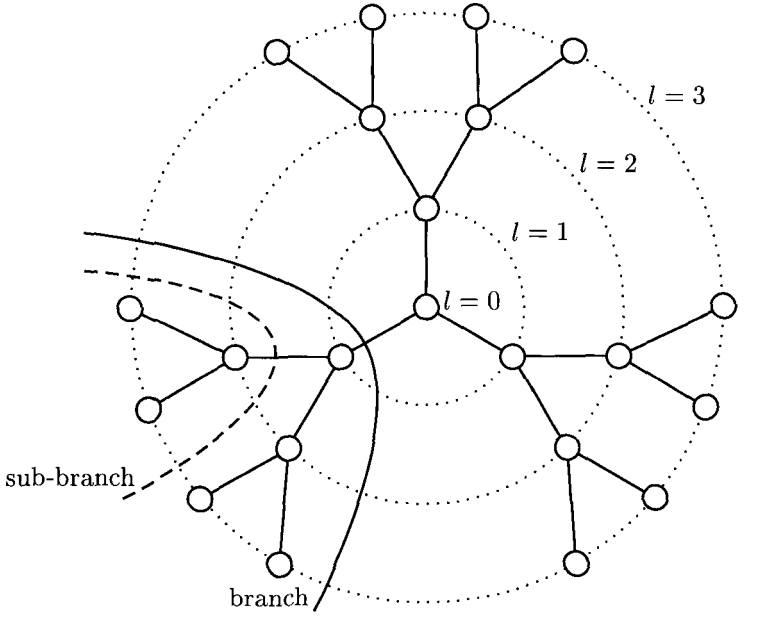

Fig. 1.7 The Bethe lattice with coordination number $z = 3$ and four generations $l = 0, 1, 2, 3$, where the parent in the centre is the 0th generation. One of the $z = 3$ branches originating from the parent in the centre is enclosed with a solid line. One of the $z-1 = 2$ sub-branches within this branch is enclosed with a dashed line. Note that for $z = 2$, the Bethe lattice is equivalent to a one-dimensional lattice.

Topologically, a Bethe lattice with $z > 2$ is different from a hyper-lattice. For example, the usual Euclidean distance cannot be naturally carried over to the Bethe lattice. However, the so-called chemical distance, that is, the length of the unique path between two sites, does provide a notion of distance that is applicable in the site-site correlation function, see Section 1.3.6. In the following, it will be convenient to refer to branches and sub-branches of a given site. In Figure 1.7, the centre site has z branches, and each branch contains $z - 1$ sub-branches. However, in infinite lattices, all sites are equivalent. For example, there is nothing special about the centre site, or, for that matter, any of the other sites displayed in Figure 1.7. Thus a sub-branch is itself a branch, and we only make the distinction for the sake of clarifying our discussion.

1.3.2 *Critical occupation probability*

The percolating cluster is equivalent to a cluster which extends indefinitely. Imagine performing a walk on the percolating infinite cluster where the retracing of steps is forbidden. At each step, there are $(z - 1)$ branches of which only $p(z - 1)$ are accessible on average. In order to continue walking on the cluster, there must be at least one accessible branch to walk along, that is,

$$p(z - 1) \geq 1. \tag{1.22}$$

Therefore, we identify the transition to percolation at

$$p_c = \frac{1}{z - 1}. \tag{1.23}$$

The critical occupation probability depends on the coordination number, z. We say that p_c is non-universal because it depends on the lattice details. Note that for $z = 2$, we recover the one-dimensional critical occupation probability $p_c = 1$. However, for $z > 2$, the critical occupation probability $p_c < 1$. In contrast to percolation in one dimension, p_c can be approached both from below and above.

1.3.3 *Average cluster size*

What is the average cluster size $\chi(p)$, to which an occupied site belongs on the Bethe lattice? Let us consider this occupied site to be the centre site of the lattice in Figure 1.7. We make use of the fact that a Bethe

lattice has no loops, and that, in an infinite lattice, all sites are equivalent, to write closed-form equations for the average cluster size. Let B denote the contribution to the average cluster size from a given branch. Then, the average cluster size, to which the occupied centre site belongs, is

$$\chi(p) = 1 + zB, \tag{1.24}$$

where the first term is the contribution from the centre site itself and the second term is the contribution from the z branches. If the parent of a branch is unoccupied, there is no contribution. If, however, the parent of a branch is occupied, that parent contributes its own weight together with a contribution B from each of its $z-1$ sub-branches. The contribution from a sub-branch is identical to the contribution from a branch because all sites are equivalent. Thus

$$B = (1-p)\,0 \; + p\,[1 + (z-1)B] \quad \text{for } 0 < p < p_c, \tag{1.25}$$

therefore

$$B = \frac{p}{1-(z-1)p} \quad \text{for } 0 < p < p_c. \tag{1.26}$$

Note that we restrict ourselves to $0 < p < p_c$ to ensure that the cluster, to which the centre belongs, is finite. Substituting B into Equation (1.24), we find that

$$\chi(p) = \frac{1+p}{1-(z-1)p} \quad \text{for } 0 < p < p_c, \tag{1.27}$$

which is consistent with the average cluster size for one-dimensional percolation when $z = 2$, see Equation (1.14). As p tends to p_c from below, the average cluster size diverges. As written in Equation (1.27), however, the way in which the average cluster size diverges is concealed. But identifying $p_c = 1/(z-1)$ and multiplying the numerator and denominator on the right-hand side of Equation (1.27) by p_c, we arrive at

$$\chi(p) = \frac{p_c(1+p)}{p_c - p} \quad \text{for } 0 < p < p_c. \tag{1.28}$$

Figure 1.8 displays the average cluster size as a function of occupation probability p for $p < 1/2$ in a Bethe lattice with $z = 3$. The average cluster size on the Bethe lattice is an increasing function of p and diverges as p

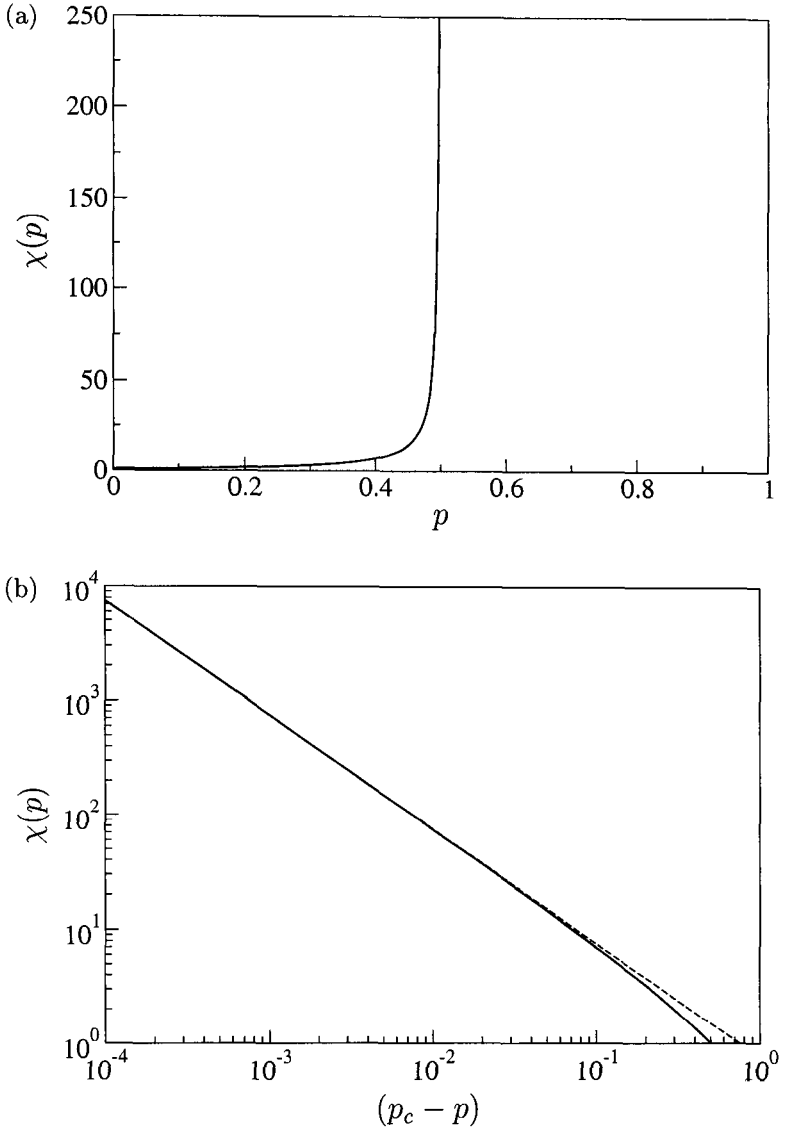

Fig. 1.8 Exact solution of the average cluster size for percolation on the Bethe lattice with $z = 3$ and $p < p_c$, where $p_c = 1/2$. (a) The average cluster size, $\chi(p)$, versus the occupation probability, p. For p approaching p_c from below, the average cluster size diverges. For p tending to zero, $\chi(p)$ tends to one. (b) The average cluster size, $\chi(p)$, versus $(p_c - p)$, the distance of p below p_c (solid line). For $p \to p_c^-$, the average cluster size diverges as a power law with exponent -1 in terms of $(p_c - p)$. The dashed straight line has slope -1.

approaches p_c from below as a power law with exponent -1 in terms of the distance of p below p_c:

$$\chi(p) = \frac{p_c(1+p)}{p_c - p} \to p_c(1+p_c)(p_c - p)^{-1} \quad \text{for } p \to p_c^-. \tag{1.29}$$

The exponent, characterising the divergence of the average cluster size as p approaches p_c is independent of the coordination number of the Bethe lattice. Thus, in contrast to p_c, the exponent is insensitive to the underlying lattice details. We say that the exponent is universal.

1.3.4 *Transition to percolation*

What is the probability $P_\infty(p)$ that a site belongs to the percolating infinite cluster? When $p \leq p_c$, there is no percolating infinite cluster, so $P_\infty(p) = 0$ for $p \leq p_c$, by definition. In order to calculate $P_\infty(p)$ for $p > p_c$, let $Q_\infty(p)$ denote the probability that a given branch does not connect to the percolating cluster. Thus, the probability that an arbitrarily selected site, for example the centre site in Figure 1.7, belongs to the percolating infinite cluster is the probability that the site is occupied, p, multiplied by the probability $1 - Q_\infty^z(p)$ that at least one of the z branches originating from this site connects to the percolating infinite cluster, that is,

$$P_\infty(p) = p\,[1 - Q_\infty^z(p)]. \tag{1.30}$$

A given branch does not connect to the percolating infinite cluster if the parent of the branch is unoccupied or, if the parent is occupied, none of the $z-1$ sub-branches connect to the percolating infinite cluster. Again, using the fact that all sites are equivalent, $Q_\infty(p)$ is also the probability that a sub-branch does not connect to the percolating infinite cluster, that is,

$$Q_\infty(p) = (1-p) + p\,Q_\infty^{z-1}(p). \tag{1.31}$$

To avoid the tedious algebra associated with solving Equation (1.31) for general z (see Exercise 1.7) we restrict ourselves to $z = 3$, where the solution to the resulting quadratic equation is

$$Q_\infty(p) = \frac{1 \pm \sqrt{(2p-1)^2}}{2p} = \begin{cases} 1 & \text{for } p \leq p_c \\ \frac{1-p}{p} & \text{for } p > p_c. \end{cases} \tag{1.32}$$

When $p \leq p_c$, there is no percolating infinite cluster, corresponding to the solution $Q_\infty(p) = 1$. When $p > p_c$, there is a percolating infinite

cluster, corresponding to the solution $Q_\infty(p) = (1-p)/p < 1$. With these identifications in mind, we substitute $Q_\infty(p)$ into Equation (1.30) to obtain

$$P_\infty(p) = \begin{cases} 0 & \text{for } p \leq p_c \\ p\left[1 - \left(\frac{1-p}{p}\right)^3\right] & \text{for } p > p_c. \end{cases} \tag{1.33}$$

The probability $P_\infty(p)$ that a site belongs to the percolating infinite cluster is a continuous function of p with $P_\infty(p) = 0$ for $p \leq p_c$ and $P_\infty(p) > 0$ for $p > p_c$, see Figure 1.9(a).

The continuous function $P_\infty(p)$, however, is not differentiable at $p = p_c$. The value p_c, at which $P_\infty(p)$ picks up, marks a transition from a non-percolating to a percolating phase, and physicists describe this phenomenon as a continuous phase transition. The parameter $P_\infty(p)$ describing the phase transition is equivalent to the fraction of lattice sites belonging to the percolating infinite cluster. It becomes non-zero for $p > p_c$ when a finite fraction of the lattice sites belong to the percolating cluster. Thus the transition gives rise to a cluster of macroscopic size.

Although $P_\infty(p)$ is not diverging (after all, probabilities cannot exceed one), we nevertheless investigate how it picks up at $p = p_c$. To extract this information, we Taylor expand $P_\infty(p)$ around $p = p_c = 1/2$, see Appendix A. The first two non-zero terms in the Taylor expansion are

$$P_\infty(p) = 6\,(p - p_c) - 24\,(p - p_c)^2 + \cdots \quad \text{for } p > p_c. \tag{1.34}$$

For p approaching p_c from above, the higher order terms become negligible and, to leading order, $P_\infty(p)$ is proportional to the distance of p above p_c, that is,

$$P_\infty(p) \propto (p - p_c) \quad \text{for } p \to p_c^+. \tag{1.35}$$

Figure 1.9(b) shows $P_\infty(p)$ versus $p - p_c$ with logarithmic axes. The graph has been divided into two portions, the left portion being well approximated by Equation (1.35), while the right portion would require higher-order terms to be reproduced faithfully. Since $P_\infty(p)$ is proportional to $(p - p_c)$ raised to the power of $+1$ for $p \to p_c^+$, the left portion is well approximated by a straight line with slope $+1$. The above analysis on the behaviour of $P_\infty(p)$ as p approaches p_c from above is not only valid for $z = 3$. Rather like the behaviour of the average cluster size for p approaching p_c, the exponent of $+1$ characterising the pick-up of $P_\infty(p)$ is universal because it is independent of the coordination number z.

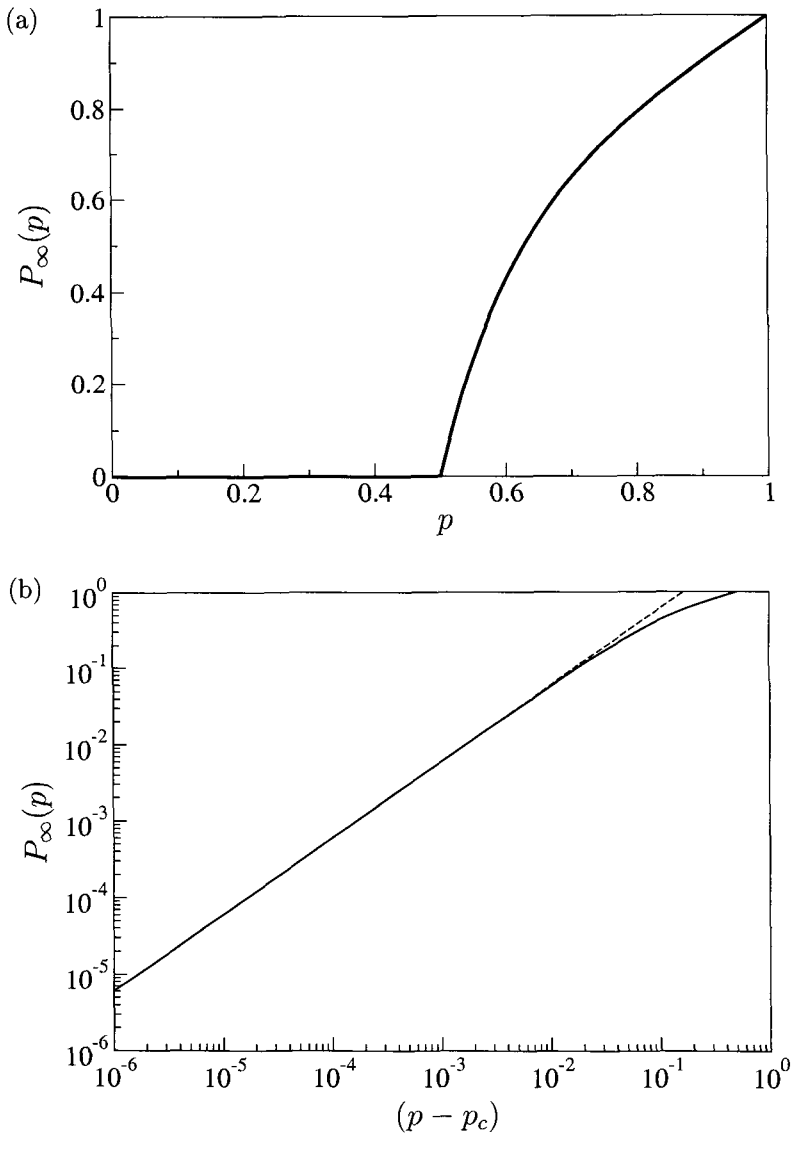

Fig. 1.9 Exact solution of the order parameter for percolation on the Bethe lattice with $z = 3$ where $p_c = 1/2$. (a) The probability, $P_\infty(p)$, that a site belongs to the percolating infinite cluster versus the occupation probability, p. For $p \leq p_c$, $P_\infty(p) = 0$ but then picks up abruptly at $p = p_c$. For $p > p_c$, a finite fraction of the sites belongs to the percolating cluster. (b) The probability, $P_\infty(p)$, versus $(p - p_c)$, the distance of p above p_c (solid line). For $p \to p_c^+$, the probability $P_\infty(p)$ picks up as a power law with exponent $+1$ in terms of $(p - p_c)$. The dashed straight line has slope $+1$.

1.3.5 *Cluster number density*

We now discuss the cluster number density for the Bethe lattice. We recall from one-dimensional percolation that $n(s,p) = (1-p)^2 p^s$, see Equation (1.2), corresponding to s occupied sites bounded by two unoccupied sites. This result can be formally generalised for clusters of any geometry.

Consider a cluster of size s and let t denote the size of the perimeter, that is, the number of unoccupied nearest neighbours of the cluster. In general, the number density of an s-cluster is not just $(1-p)^t p^s$, since s-clusters may neither have a unique geometry (possibly leading to a different number of perimeter sites t) nor a unique orientation. Introducing a degeneracy factor, $g(s,t)$, to count the number of different clusters of size s and perimeter t, the cluster number density can be expressed as

$$n(s,p) = \sum_{t=1}^{\infty} g(s,t)\,(1-p)^t p^s, \tag{1.36}$$

where the sum is performed over all possible perimeters t.

In one dimension, an s-cluster has a unique geometry and orientation with $t = 2$ for all s and

$$g(s,t) = \begin{cases} 0 & \text{for } t \neq 2 \\ 1 & \text{for } t = 2, \end{cases} \tag{1.37}$$

thus recovering Equation (1.2). In the Bethe lattice, $g(s,t)$ is not as trivial.

Figure 1.10 shows two clusters of size $s = 4$ with different geometries. We note that both clusters have $t = 6$ perimeter sites. The Bethe lattice enjoys the simplification that all clusters of size s have the same number of perimeter sites $t = 2 + s(z-2)$. The one-to-one correspondence between the cluster size s and perimeter sites t on the Bethe lattice reduces the sum in Equation (1.36) to a single term, so that

$$n(s,p) = g[s, 2+s(z-2)]\,(1-p)^{2+s(z-2)} p^s. \tag{1.38}$$

For coordination number $z = 3$, Equation (1.38) becomes

$$n(s,p) = g(s, 2+s)\,(1-p)^{2+s} p^s \quad \text{for } z = 3. \tag{1.39}$$

It is, in fact, possible to enumerate $g(s, 2+s)$ by the use of generating functions, see e.g. [Fisher and Essam, 1961], but for our purposes we proceed more simply. To avoid enumerating $g(s, 2+s)$, we study the relative changes of the cluster number density around p_c. In this way, the degeneracy factor

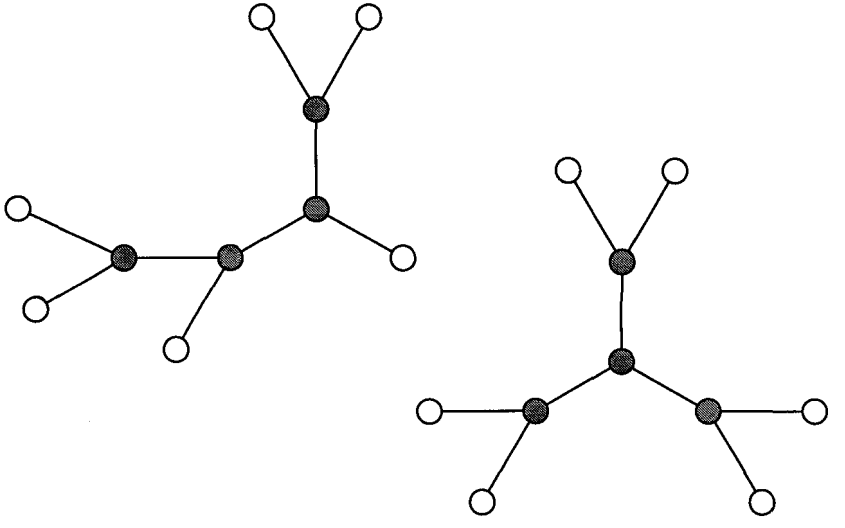

Fig. 1.10 Two different clusters of size $s = 4$ for site percolation on a Bethe lattice with $z = 3$. Occupied sites are dark grey while unoccupied sites are white. The perimeter, t, is the number of unoccupied nearest neighbours of a cluster. For both clusters, the perimeter $t = 2 + s = 6$.

$g(s, 2+s)$ cancels out, and we find

$$\begin{aligned}\frac{n(s,p)}{n(s,p_c)} &= \left[\frac{1-p}{1-p_c}\right]^2 \left[\frac{(1-p\,)\,p}{(1-p_c)\,p_c}\right]^s \\ &= \left[\frac{1-p}{1-p_c}\right]^2 \exp\left(s \ln\left[\frac{(1-p\,)\,p}{(1-p_c)\,p_c}\right]\right) \\ &= \left[\frac{1-p}{1-p_c}\right]^2 \exp\left(-s/s_\xi\right), \end{aligned} \tag{1.40}$$

where we have defined the characteristic cluster size

$$s_\xi(p) = -\frac{1}{\ln\left[\frac{(1-p\,)\,p}{(1-p_c)\,p_c}\right]}. \tag{1.41}$$

Figure 1.11(a) displays the characteristic cluster size $s_\xi(p)$ versus occupation probability p on the Bethe lattice with $z = 3$ where $p_c = 1/2$. When p approaches p_c, the characteristic cluster size diverges. The characteristic cluster size decreases with p when $p > p_c$ since it is a measure of the typical size of the largest finite cluster.

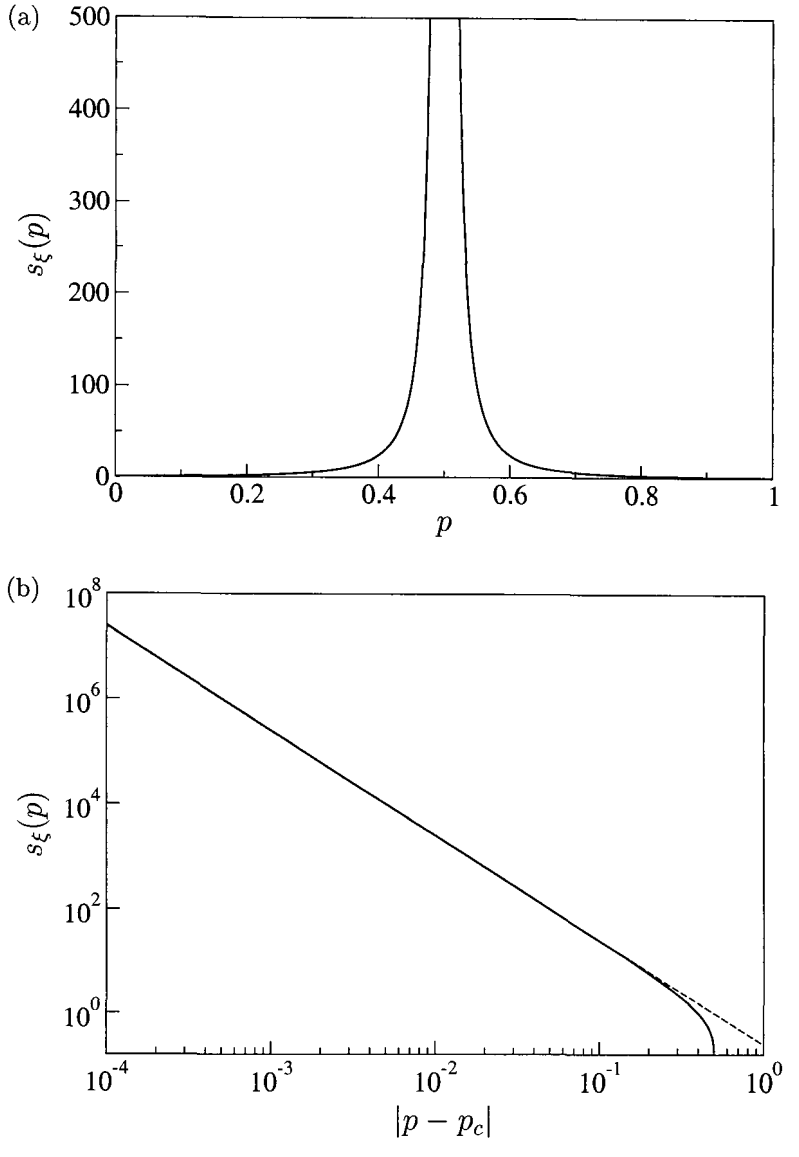

Fig. 1.11 Exact solution of the characteristic cluster size for percolation on the Bethe lattice with $z = 3$ where $p_c = 1/2$. (a) The characteristic cluster size, $s_\xi(p)$, versus the occupation probability, p. For p approaching p_c, the characteristic cluster size diverges. For p tending to zero or one, $s_\xi(p)$ tends to zero. (b) The characteristic cluster size, $s_\xi(p)$, versus $|p - p_c|$, the distance of p from p_c (solid line). For $p \to p_c$, the characteristic cluster size diverges as a power law with exponent -2 in terms of $(p - p_c)$. The dashed straight line has slope -2.

To extract how the characteristic cluster size $s_\xi(p)$ diverges for p approaching p_c (both from below and above), we rework the argument of the logarithm, using $p_c = 1/2$:

$$\begin{aligned} s_\xi(p) &= -\frac{1}{\ln\left[\frac{(1-p)\,p}{(1-p_c)\,p_c}\right]} \\ &= -\frac{1}{\ln[4p - 4p^2]} \\ &= -\frac{1}{\ln[1 - 4(p-p_c)^2]} \\ &\to \frac{1}{4}\,(p-p_c)^{-2} \qquad \text{for } p \to p_c. \end{aligned} \tag{1.42}$$

Thus the characteristic cluster size $s_\xi(p)$ diverges as a power law with exponent -2 in terms of $(p - p_c)$, the distance of p from $p_c = 1/2$, see Figure 1.11(b).

Rearranging Equation (1.40), we find that the cluster number density at occupation probability p is

$$n(s,p) = \left[\frac{1-p}{1-p_c}\right]^2 n(s,p_c)\exp\left(-s/s_\xi\right), \tag{1.43a}$$

$$s_\xi(p) = -\frac{1}{\ln\left[\frac{(1-p)\,p}{(1-p_c)\,p_c}\right]}, \tag{1.43b}$$

where the characteristic cluster size is given as in Equation (1.41). Note that for p approaching p_c, the characteristic cluster size $s_\xi(p)$ diverges so that the exponential becomes equal to one, guaranteeing the consistency of Equation (1.43a) at $p = p_c$.

Now we have to consider the behaviour of $n(s,p_c)$, the cluster number density at p_c. For the final word on $n(s,p_c)$, we refer the reader to [Fisher and Essam, 1961]; however, there are strong constraints that can be imposed on $n(s,p_c)$. First, according to Equation (1.17), the probability that a site belongs to a finite cluster, $\sum_{s=1}^{\infty} sn(s,p)$, is finite, see Figure 1.12. Second, the average cluster size

$$\chi(p) = \frac{\sum_{s=1}^{\infty} s^2 n(s,p)}{\sum_{s=1}^{\infty} sn(s,p)} \quad \text{for } 0 < p < 1 \tag{1.44}$$

diverges as p approaches p_c from below, see Equation (1.29). But since the denominator is finite, the numerator itself must diverge.

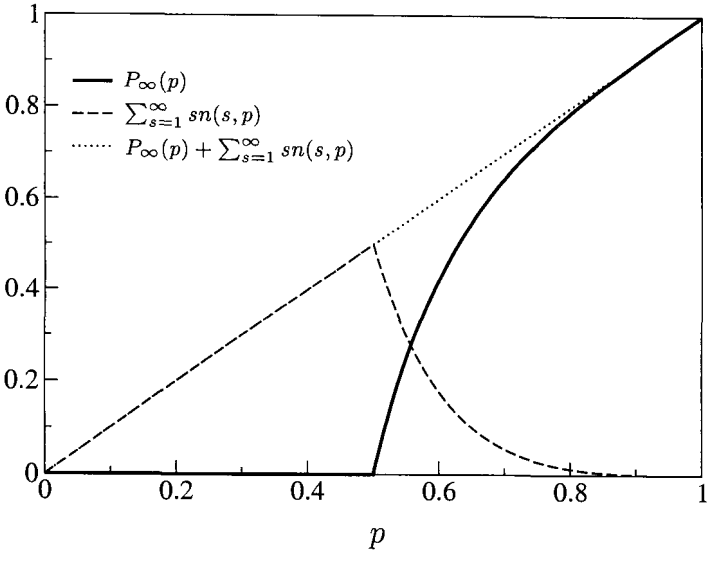

Fig. 1.12 Exact results for percolation on the Bethe lattice with $z = 3$ where $p_c = 1/2$. The probability, $P_\infty(p)$, that a site belongs to the percolating infinite cluster (solid line), added to the probability, $\sum_{s=1}^{\infty} sn(s,p)$, that the site belongs to a finite cluster (dashed line) equals the probability, p, that the site is occupied (dotted line). Note that when $p \leq p_c$, the sum over finite clusters $\sum_{s=1}^{\infty} sn(s,p_c) = p$, since $P_\infty(p) = 0$.

In summary, $n(s,p_c)$ must satisfy the constraints

$$\sum_{s=1}^{\infty} sn(s,p_c) = p_c - P_\infty(p_c), \tag{1.45a}$$

$$\sum_{s=1}^{\infty} s^2 n(s,p) \to \infty \quad \text{for } p \to p_c. \tag{1.45b}$$

Although these two constraints do not uniquely determine the form of $n(s,p_c)$, a power-law decay, $n(s,p_c) \propto s^{-\tau}$ for $s \gg 1$, is not only consistent with the two constraints in Equation (1.45) if the exponent $2 < \tau \leq 3$, but is also consistent with the exact cluster number density displayed in Figure 1.13(a). For large cluster sizes, the power-law decay of the cluster number density with exponent $\tau = 5/2$ can be proved rigorously, as we shall see in Section 3.4.

Note that in one dimension, the cluster number density equals zero at p_c and does not decay like a power law. Therefore, the lower constraint $2 < \tau$, originating from Equation (1.45a), does not apply. Collecting all these

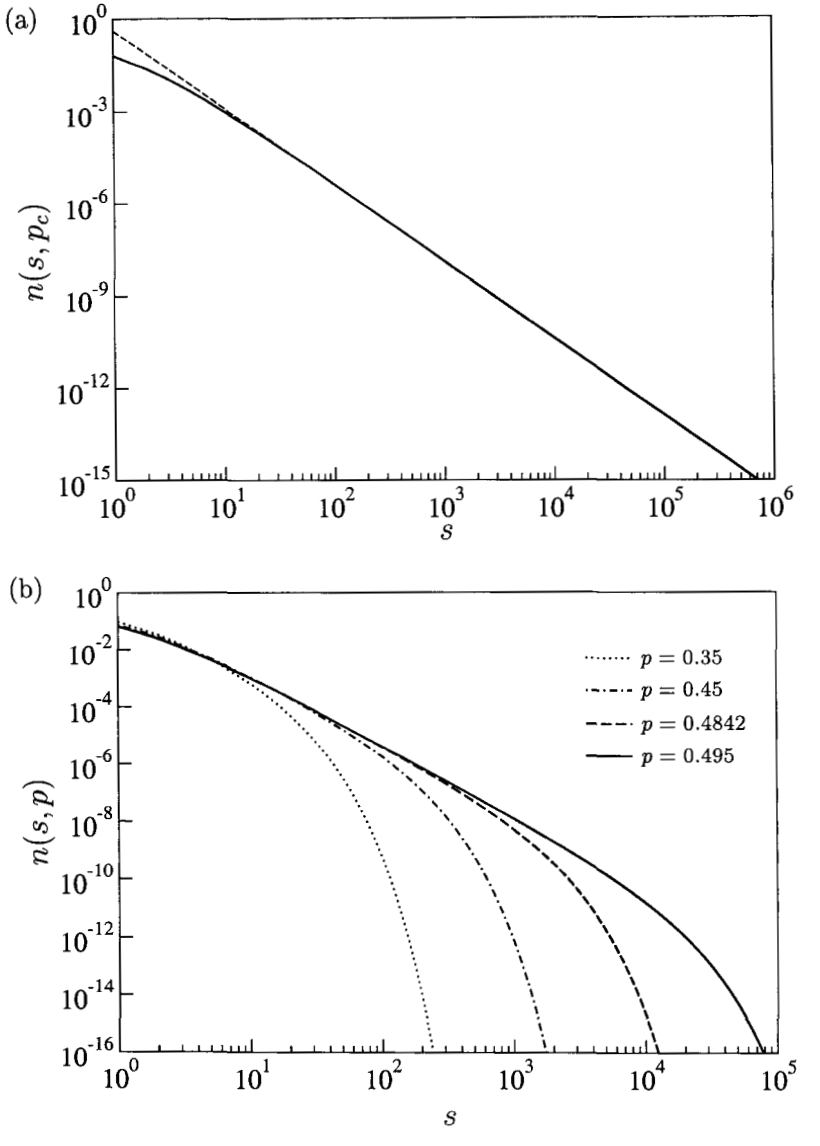

Fig. 1.13 Exact solution of the cluster number density for percolation on the Bethe lattice with $z = 3$ where $p_c = 1/2$. (a) The cluster number density, $n(s, p_c)$, versus the cluster size, s. For large cluster sizes, the cluster number density is well approximated by a power-law decay, $n(s, p_c) \propto s^{-\tau}$ for $s \gg 1$, with exponent $\tau = 5/2$. The dashed straight line has slope $-5/2$. (b) The cluster number density, $n(s, p)$, versus the cluster size, s. The four curves correspond to $p = 0.35, 0.45, 0.4842, 0.495$ with characteristic cluster sizes $s_\xi(p) \approx 10, 100, 1\,000, 10\,000$, respectively.

results together, the cluster number density $n(s,p)$ for the Bethe lattice is approximately of the form

$$n(s,p) \propto s^{-\tau} \exp(-s/s_\xi) \quad \text{for } s \gg 1, p \to p_c, \tag{1.46a}$$

$$s_\xi(p) \propto (p-p_c)^{-2} \quad \text{for } p \to p_c, \tag{1.46b}$$

where the characteristic cluster size diverges as a power law with exponent -2 in terms of $(p-p_c)$, when p tends to p_c.

In Figure 1.13(b) we display the exact solutions of the cluster number density versus the cluster size for four different values of occupation probabilities, $p = 0.35, 0.45, 0.4842, 0.495$. Each graph for the cluster number density has a characteristic cluster size, which is the typical size of the largest cluster in a realisation. From Equation (1.43b), we find that $s_\xi(p) \approx 10, 100, 1\,000, 10\,000$, respectively. For p approaching p_c and cluster sizes $s \ll s_\xi$, the cluster number density decays approximately as a power law in s, that is, $n(s,p) \propto s^{-\tau}$, while decaying faster than a power law for $s \gg s_\xi$. The graph corresponding to $p = p_c$ in Figure 1.13(a) is qualitatively different. There is no characteristic cluster size because $s_\xi(p_c) = \infty$. Thus, there are two distinct behaviours: for $p \neq p_c$, there exists a finite characteristic cluster size, which diverges for p approaching p_c, while at $p = p_c$, the characteristic cluster size is infinite.

As another test for the validity of the scaling form in Equation (1.46), we may calculate the average cluster size, $\chi(p)$, in terms of the cluster number density, by using Equation (1.44):

$$\begin{aligned}
\chi(p) &= \frac{\sum_{s=1}^{\infty} s^2 n(s,p)}{\sum_{s=1}^{\infty} s n(s,p)} \\
&\propto \sum_{s=1}^{\infty} s^{2-\tau} \exp(-s/s_\xi) \\
&\approx \int_1^{\infty} s^{2-\tau} \exp(-s/s_\xi)\, ds \\
&= \int_{1/s_\xi}^{\infty} (u s_\xi)^{2-\tau} \exp(-u) s_\xi\, du \quad \text{with } u = s/s_\xi \\
&= s_\xi^{3-\tau} \int_{1/s_\xi}^{\infty} u^{2-\tau} \exp(-u)\, du,
\end{aligned} \tag{1.47}$$

where we have replaced the sum by an integral and made the substitution $u = s/s_\xi$. Letting p tend to p_c, the characteristic cluster size $s_\xi(p)$ diverges and the lower limit of the integral tends to zero. This integral is frequently

encountered and is none other than the Gamma function

$$\Gamma(x) = \int_0^\infty u^{x-1} \exp(-u)\, du. \tag{1.48}$$

In our case, $x = 3 - \tau$ and the integral is just the number $\Gamma(3 - \tau)$. Thus the average cluster size $\chi(p)$ diverges like the characteristic cluster size $s_\xi(p)$ raised to the power $3 - \tau$. Equations (1.29) and (1.42) characterise, respectively, how $\chi(p)$ and $s_\xi(p)$ diverge when p tends to p_c^-. Therefore

$$\begin{aligned} \chi(p) &\propto (p_c - p)^{-1} \\ &\propto s_\xi^{3-\tau} \\ &\propto (p_c - p)^{2\tau-6} \quad \text{for } p \to p_c^-, \end{aligned} \tag{1.49}$$

so we identify $\tau = 5/2$, which satisfies the constraint $2 < \tau \leq 3$ and is consistent with the power-law decay for large cluster sizes of the exact solution for the cluster number density displayed in Figure 1.13(a).

1.3.6 *Correlation function*

Given that a site i is occupied, the probability that a particular site j, l generations away, is occupied and belongs to the same finite cluster is the site-site correlation function, $g(i, j)$. Since there is a unique path between the sites i and j, $g(i, j) = p^l$. In the Bethe lattice, there is no Euclidean distance function between two general sites. However, treating site i as the parent in the centre of the Bethe lattice, the generation number of the site j provides a reasonable notion of distance. Accordingly, it is natural to calculate the average number of sites, $N(i; l)$, situated $l \geq 1$ generations away, that are occupied and belong to the same finite cluster as the parent site i in the centre. The expected number $N(i; l)$ is obtained by summing the site-site correlation function over all sites in the lth generation, that is,

$$N(i; l) = \sum_{j \in l} g(i, j) = n(l)p^l \quad \text{for } l \geq 1, \tag{1.50}$$

where $n(l)$ is the number of sites in the lth generation. In a Bethe lattice with coordination number z, each branch has $(z - 1)^{l-1}$ sites in the lth generation. Since the parent in the centre provides z branches, there are in total $n(l) = z(z - 1)^{l-1}$ sites in the lth generation. Therefore,

$$N(i; l) = z(z - 1)^{l-1}p^l \quad \text{for } l \geq 1. \tag{1.51}$$

Restricting ourselves to $0 < p < p_c$, we can characterise the decay in the expected number of sites in the lth generation belonging to the same finite cluster as the parent in the centre in the time-honoured fashion

$$\begin{aligned} N(i;l) &= \frac{z}{z-1}[(z-1)p]^l \quad \text{for } 0 < p < p_c \\ &= \frac{z}{z-1}\exp(-l/l_\xi) \quad \text{for } 0 < p < p_c, l \geq 1, \end{aligned} \tag{1.52}$$

where we have defined a characteristic generation

$$l_\xi(p) = -\frac{1}{\ln([z-1]p)} = -\frac{1}{\ln(p/p_c)} \quad \text{for } 0 < p < p_c, l \geq 1. \tag{1.53}$$

The characteristic generation $l_\xi(p)$ diverges for p approaching p_c from below, so that the exponential term in Equation (1.52) becomes one at $p = p_c$, leaving $N(i;l) = z/(z-1)$, independent of the generation l.

We can recover the average cluster size Equation (1.27) for $p < p_c$ by summing the site-site correlation function, $g(i,j)$, over all possible sites j,

$$\begin{aligned} \sum_j g(i,j) &= g(i,i) + \sum_{j \neq i} g(i,j) \\ &= 1 + \sum_{l=1}^{\infty} N(i;l) \\ &= 1 + \sum_{l=1}^{\infty} \frac{z}{z-1}[(z-1)p]^l \\ &= 1 + \frac{z}{(z-1)}\frac{(z-1)p}{1-(z-1)p} \quad \text{for } 0 < p < p_c \\ &= \frac{1+p}{1-(z-1)p} \quad \text{for } 0 < p < p_c \\ &= \chi(p) \quad \text{for } 0 < p < p_c. \end{aligned} \tag{1.54}$$

The 'sum rule' in Equation (1.54) and the equivalent sum rule in one dimension in Equation (1.21) are special cases of a very general result known as the fluctuation-dissipation theorem.

1.4 Percolation in $d = 2$

The reader is now familiar with the techniques for extracting quantities of interest from the cluster number density such as the average cluster size and the characteristic cluster size. We have also been able to locate

the transition to percolation by explicitly calculating the critical occupation probability. Furthermore, we have characterised the behaviour of the above quantities in the vicinity of the phase transition. We found that the location of the phase transition is dependent on the underlying lattice details, while the exponents characterising the behaviour of $\chi(p)$, $s_\xi(p)$, and $P_\infty(p)$, near p_c, are not.

The exact results obtained thus far for the one-dimensional lattice and the Bethe lattice relied heavily on there being no loops. However, in general, clusters may form loops, making exact analytic results impossible but for a few special cases. Our programme now is to focus on percolation in two dimensions, which is nontrivial, motivating a more general approach to percolation [Stauffer and Aharony, 1994]. In doing so, we will lay the foundations for a general framework to encompass the phenomena encountered close to the continuous percolation phase transition. As we shall see later, this general framework can be applied to all systems exhibiting a continuous phase transition.

1.4.1 *Transition to percolation*

In one-dimensional percolation, the critical occupation probability $p_c = 1$, while for percolation on a Bethe lattice $p_c = 1/(z-1) < 1$ for coordination number $z > 2$. What is the critical occupation probability in two-dimensional site percolation on a square lattice? Looking back at Figure 1.2, a good guess would be p_c around 0.59. There is in fact no exact result for p_c on a square lattice, but numerics have closed in on $p_c = 0.59274621$ [Newman and Ziff, 2000]. For $p > p_c$ there is a single percolating cluster, while for $p \leq p_c$ there is no percolating cluster.

What is the probability that a site belongs to the percolating cluster? Figure 1.14(a) shows the numerically measured $P_\infty(p)$ for a finite lattice of size $L = 5\,000$. For finite lattice sizes, $P_\infty(p) > 0$ for $0 < p \leq p_c$. This is a finite-size effect. However, for increasing lattice size, the pick-up in $P_\infty(p)$ approaches p_c and for $L \to \infty$ we have $P_\infty(p) = 0$ for $p \leq p_c$.

Following the terminology of continuous phase transitions, we refer to $P_\infty(p)$ as the order parameter for percolation and to p_c as the critical point. The way that the order parameter picks up at the critical point $p = p_c$ is characterised by the critical exponent β, where

$$P_\infty(p) \propto (p - p_c)^\beta \quad \text{for } p \to p_c^+. \tag{1.55}$$

For the Bethe lattice with $z > 2$, the critical exponent $\beta = 1$, while for

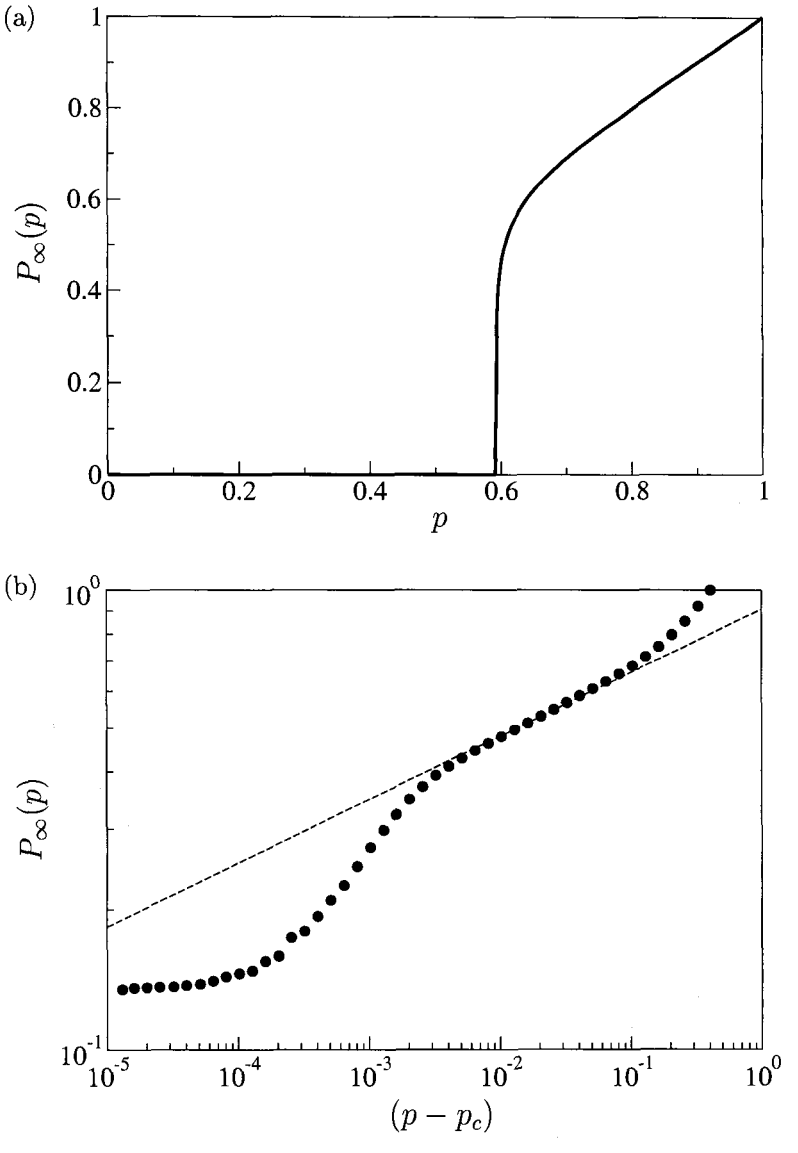

Fig. 1.14 Numerical results for the order parameter for two-dimensional site percolation on a square lattice of size $L = 5\,000$ where $p_c = 0.59274621$. (a) The order parameter, $P_\infty(p)$, versus the occupation probability, p. When $L \to \infty$, $P_\infty(p) = 0$ for $p \leq p_c$ but then picks up abruptly at $p = p_c$. For $p > p_c$, a finite fraction of the sites belong to the percolating cluster. (b) The order parameter, $P_\infty(p)$, versus $(p - p_c)$, the distance of p above p_c (solid circles). For $p \to p_c^+$, $P_\infty(p)$ picks up as a power law with exponent $\beta = 5/36$ in terms of $(p - p_c)$ when $L \to \infty$. The dashed straight line has slope 5/36.

two-dimensional percolation, theory gives $\beta = 5/36$, independent of the underlying lattice (e.g. square, triangular or hexagonal), see for example [Grimmett, 1999; Francesco *et al.*, 2001]. We will later justify the universality of β, that is, its insensitivity to the underlying lattice details.

In Figure 1.14(b) we attempt to confirm this theoretical value of β by plotting $\log P_\infty(p)$ against $\log(p - p_c)$ for $p > p_c$ measured in a finite lattice of size $L = 5\,000$. Without prior knowledge of the value of β, our attempt to measure it numerically would have failed, since the data do not follow an unambiguous straight line. It is, in fact, difficult to determine the critical exponent for the order parameter directly. In Section 1.8, we will develop a more powerful method for determining β, along with other critical exponents.

1.4.2 *Average cluster size*

Recalling Figure 1.2, we had the impression that the average cluster size increased with increasing $p < p_c$ before falling off for $p > p_c$. Bearing in mind that the average cluster size, by definition, only includes finite (non-percolating) clusters, the decrease for $p > p_c$ is due to the percolating cluster leaving less and less space for finite clusters.

Figure 1.15(a) shows the numerically measured average cluster size $\chi(p)$ for a square lattice of size $L = 5\,000$. For finite lattice sizes, the average cluster size cannot diverge at $p = p_c$. This is a finite-size effect. The divergence is capped by a maximum which increases with lattice size. For $L \to \infty$, the average cluster size $\chi(p)$ diverges for $p \to p_c$ as a power law with critical exponent $-\gamma$ in terms of the distance of p from p_c, that is,

$$\chi(p) \propto |p - p_c|^{-\gamma} \quad \text{for } p \to p_c. \tag{1.56}$$

For the Bethe lattice, the critical exponent $\gamma = 1$, while for two-dimensional percolation, theory gives $\gamma = 43/18$, independent of the lattice details.

In Figure 1.15(b) we attempt to confirm this theoretical value of γ by plotting $\log \chi(p)$ against $\log|p - p_c|$ for $p < p_c$ and $p > p_c$ measured in a finite lattice of size $L = 5\,000$. The data corresponding to $p < p_c$ apparently lie on a straight line for two orders of magnitude in $(p_c - p)$ before saturating because of the finiteness of the system. However, comparison with the theoretical dotted line shows that we have been misled into extracting an erroneous value for the critical exponent γ. In Section 1.8, we will describe the aforementioned method for determining critical exponents reliably.

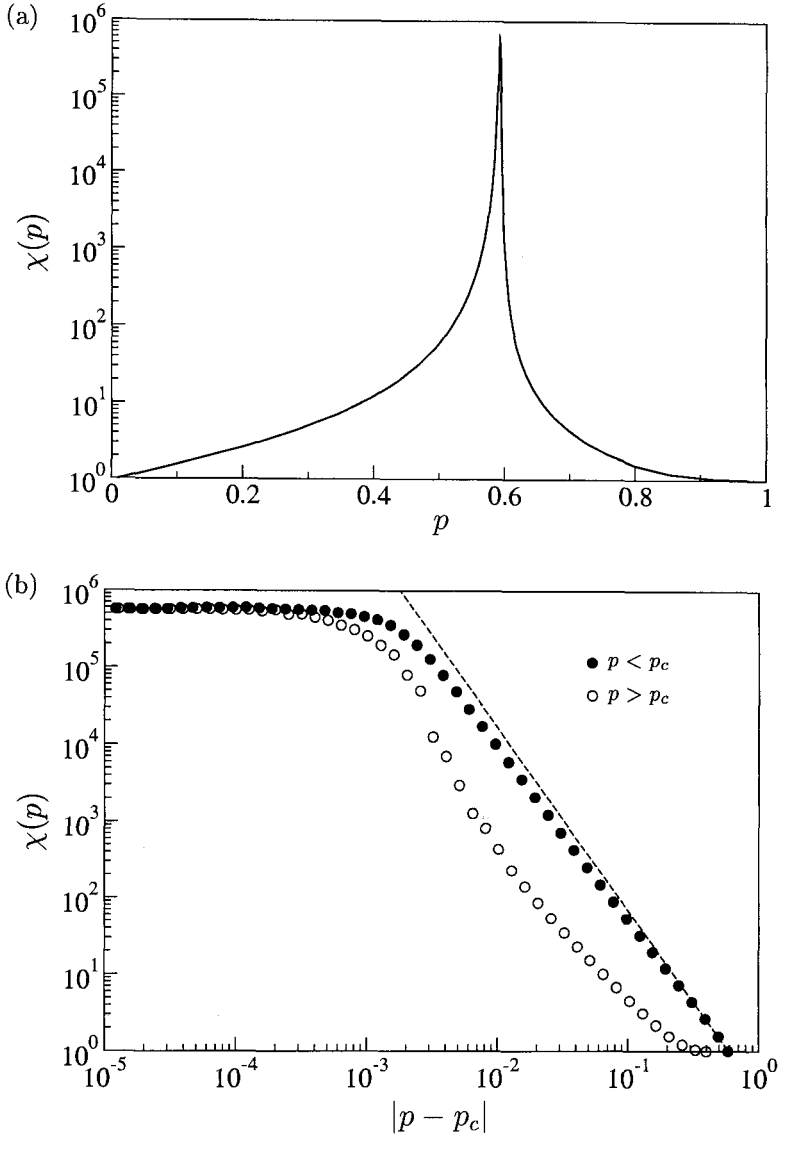

Fig. 1.15 Numerical results for the average cluster size for two-dimensional site percolation on a square lattice of size $L = 5\,000$ where $p_c = 0.59274621$. (a) The average cluster size, $\chi(p)$, versus the occupation probability, p. For $p \to p_c$, the average cluster size diverges but for finite lattices, the divergence is capped. For p tending to zero or one, $\chi(p)$ tends to one. (b) The average cluster size, $\chi(p)$, versus $|p - p_c|$, the distance of p from p_c. When $L \to \infty$, the average cluster size diverges as a power law $\chi(p) \propto |p - p_c|^{-\gamma}$ for $p \to p_c$ with $\gamma = 43/18$. The dashed straight line has slope $-43/18$.

1.4.3 *Cluster number density – exact*

Despite the above warnings, we will attempt to find the exact expression for the cluster number density in two-dimensional site percolation. Our starting point is the general form

$$n(s,p) = \sum_{t=1}^{\infty} g(s,t)\,(1-p)^t p^s, \tag{1.57}$$

where $g(s,t)$ is the number of different clusters of size s with perimeter t. Unfortunately, unlike on the Bethe lattice, there is no unique relationship between the size of a cluster, s, and the perimeter t. Nevertheless, we can enumerate $g(s,t)$ by hand for small cluster sizes, see Figure 1.16. Thus for site percolation in a two-dimensional square lattice,

$$\begin{aligned}
n(1,p) &= (1-p)^4\,p \\
n(2,p) &= 2(1-p)^6\,p^2 \\
n(3,p) &= [2(1-p)^8 + 4(1-p)^7]\,p^3 \\
n(4,p) &= [2(1-p)^{10} + 8(1-p)^9 + 9(1-p)^8]\,p^4 \\
n(5,p) &= [2(1-p)^{12} + 12(1-p)^{11} + 28(1-p)^{10} + 20(1-p)^9 + (1-p)^8]\,p^5
\end{aligned} \tag{1.58}$$

are the exact solutions of the cluster number density for clusters up to size $s = 5$.

The number $\sum_t g(s,t)$ of different clusters of size s has been tabulated up to $s = 53$, while $g(s,t)$ itself has been tabulated up to $s = 40$ [Jensen, 2001]. The exact solutions of the cluster number density up to $s = 40$ are shown in Figure 1.17. We cannot construct a theory of percolation based on clusters up to size $s = 40$ – we must consider clusters of all sizes. Therefore, we must abandon our current approach and recognise that we cannot work out the exact solutions of the cluster number density for all cluster sizes.

1.4.4 *Cluster number density – numerical*

Since exact solutions are not available for large cluster sizes, we resort to a numerical approach to obtain the general form of the cluster number density $n(s,p)$ for any s and p.

Figure 1.18(a) shows numerical results for four different values of occupation probabilities, $p = 0.54, 0.55, 0.56, 0.57$. Each graph has a characteristic cluster size $s_\xi(p)$, which is the typical size of the largest cluster in a realisation, see Figure 1.2. For all cluster sizes $s \ll s_\xi$, the cluster number

1

t	$g(1,t)$
4	1

2

t	$g(2,t)$
6	2

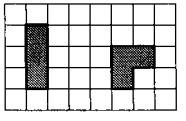

2 4

t	$g(3,t)$
8	2
7	4

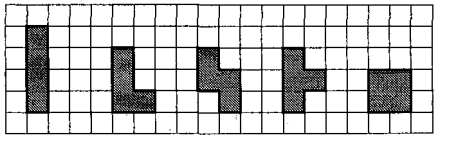

2 8 4 4 1

t	$g(4,t)$
10	2
9	8
8	9

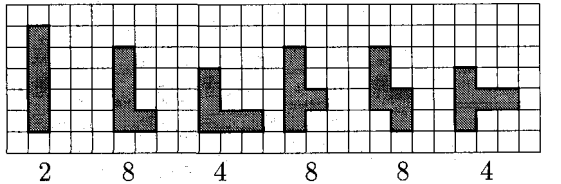

2 8 4 8 8 4

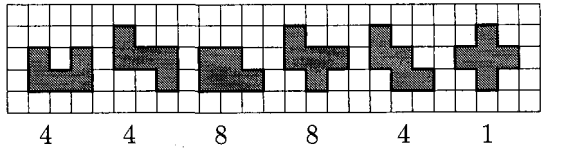

4 4 8 8 4 1

t	$g(5,t)$
12	2
11	12
10	28
9	20
8	1

Fig. 1.16 The different clusters of size $s = 1, 2, 3, 4, 5$ for two-dimensional site percolation on a square lattice. Note that there are different perimeters, t, for a given cluster size when $s \geq 3$.

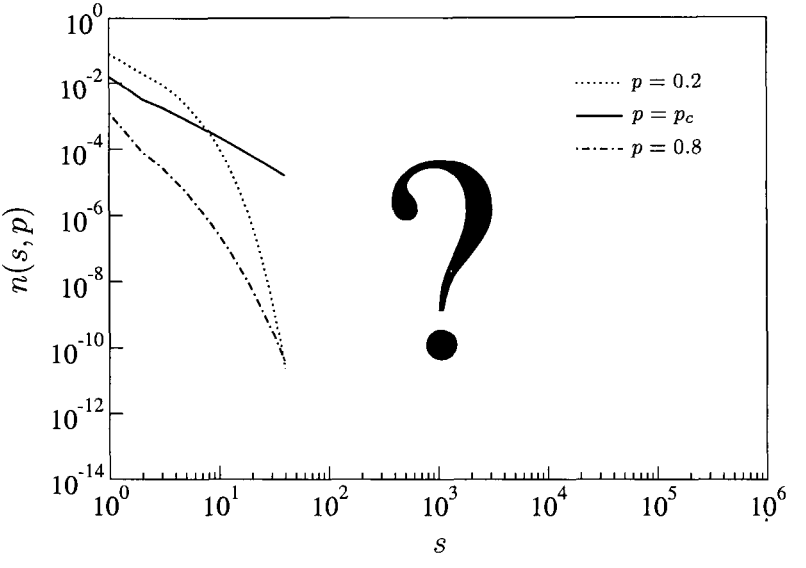

Fig. 1.17 Exact solution of the cluster number density, $n(s,p)$, versus the cluster size, s, up to size $s = 40$ for two-dimensional site percolation on a square lattice. The three curves correspond to occupation probabilities $p = 0.2, 0.59274621, 0.8$. No exact solutions are currently available above $s = 40$. Data courtesy of Dr Iwan Jensen, University of Melbourne, Australia.

density decays approximately as a power law in s, that is, $n(s,p) \propto s^{-\tau}$, while decaying faster than a power law for $s \gg s_\xi$. In the Bethe lattice, the critical exponent $\tau = 5/2$, while in two-dimensional percolation $\tau = 187/91$, independent of lattice details.

The graph corresponding to $p = p_c$ in Figure 1.18(b) is qualitatively different. There is apparently no characteristic cluster size. There are two distinct behaviours: for $p \neq p_c$, there exists a finite characteristic cluster size, which diverges for p approaching p_c, while at $p = p_c$, the characteristic cluster size is infinite. Just as in one-dimensional percolation and on the Bethe lattice, the characteristic cluster size $s_\xi(p)$ diverges as a power law with critical exponent $-1/\sigma$ in terms of the distance of p from p_c, that is,

$$s_\xi(p) \propto |p - p_c|^{-1/\sigma} \quad \text{for } p \to p_c. \tag{1.59}$$

For one-dimensional percolation, the critical exponent $\sigma = 1$, for the Bethe lattice with $z > 2$, $\sigma = 1/2$, while for two-dimensional percolation, theory gives $\sigma = 36/91$, independent of the lattice details.

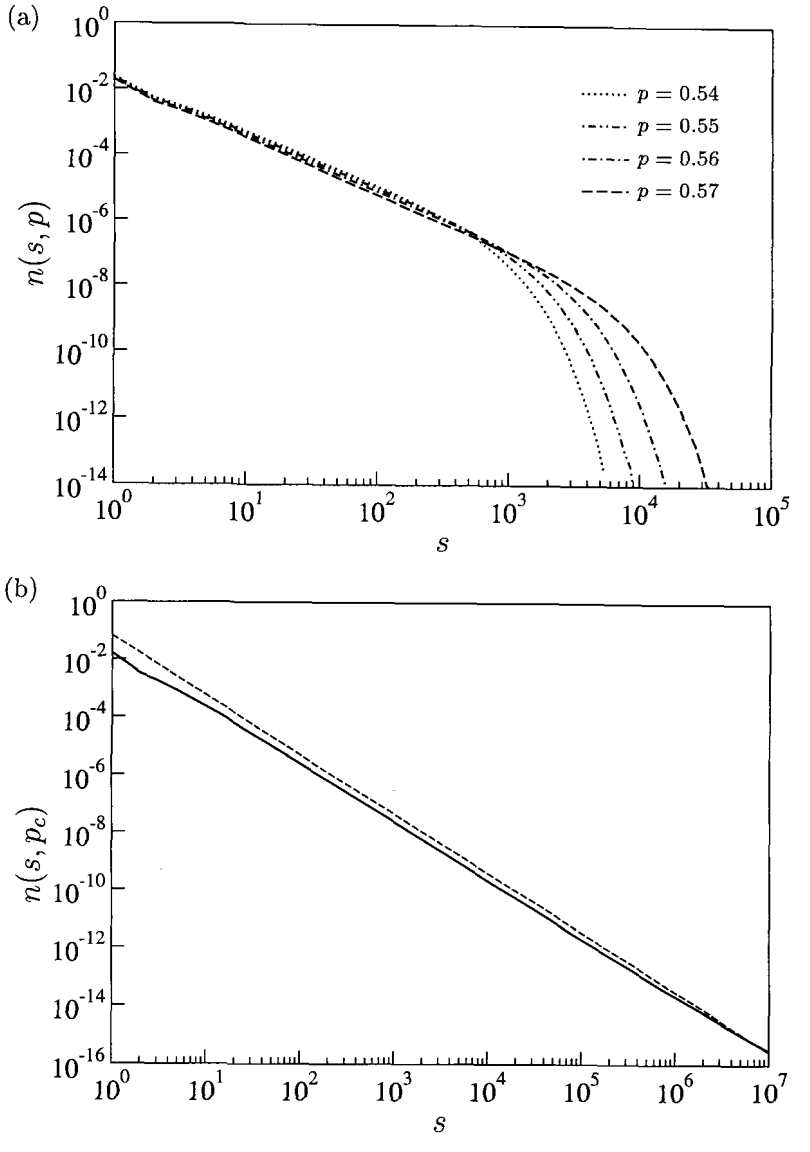

Fig. 1.18 Numerical results for the cluster number density, $n(s,p)$, versus the cluster size, s, for two-dimensional site percolation on a square lattice of size $L = 5\,000$ where $p_c = 0.59274621$. (a) For occupation probabilities $p = 0.54, 0.55, 0.56, 0.57$, the characteristic cluster size is finite and $n(s,p)$ decays as a power law for $1 \ll s \ll s_\xi$ and rapidly for $s \gg s_\xi$.(b) At $p = p_c$, the characteristic cluster size is infinite and for large cluster sizes, the cluster number density is well approximated by a power-law decay, $n(s,p_c) \propto s^{-\tau}$ for $s \gg 1$, with $\tau = 187/91$. The dashed straight line has slope $-187/91$.

1.5 Cluster Number Density – Scaling Ansatz

Since we are not able to calculate the cluster number density exactly for two-dimensional percolation for large clusters, we gather numerical evidence for the form of $n(s,p)$. There are two distinct behaviours of $n(s,p)$, depending on whether $p \neq p_c$ or $p = p_c$.

For $p \neq p_c$, there is a finite characteristic cluster size and, for a given occupation probability p, the characteristic cluster size $s_\xi(p)$ marks the crossover between a power-law decay and a rapid decay of $n(s,p)$, qualitatively,

$$n(s,p) \propto \begin{cases} s^{-\tau} & \text{for } 1 \ll s \ll s_\xi \\ \text{decays rapidly} & \text{for } s \gg s_\xi. \end{cases} \tag{1.60}$$

When p approaches p_c, the critical exponent σ determines how the characteristic cluster size diverges, see Equation (1.59).

For $p = p_c$, the characteristic cluster size is infinite, so that for any finite cluster, $s \ll s_\xi$. Therefore, the cluster number density decays as a power law for large cluster sizes

$$n(s,p_c) \propto s^{-\tau} \quad \text{for } s \gg 1, \tag{1.61}$$

except in one dimension where $n(s,p_c) = 0$.

With this qualitative picture in mind, and drawing on the results for the Bethe lattice, we propose the following scaling ansatz[1] for the cluster number density

$$n(s,p) \propto s^{-\tau} \exp\left(-s/s_\xi\right) \quad \text{for } p \to p_c, s \gg 1, \tag{1.62a}$$

$$s_\xi(p) \propto |p - p_c|^{-1/\sigma} \quad \text{for } p \to p_c, \tag{1.62b}$$

where the characteristic cluster size diverges like a power law in terms of the distance of p from p_c.

Evidently, the proposed ansatz encompasses the Bethe lattice. If our ansatz is to be general, it must also include the exact solutions of the trivial one-dimensional lattice and the numerical results for two-dimensional lattices. Recalling the results for the cluster number density and the characteristic cluster size in one dimension, we update Equation (1.3) and Equa-

[1] A 'scaling ansatz' is synonymous with a 'scaling hypothesis' and refers to a proposition that has not been derived analytically, but is consistent with known data. For distinction, we will reserve the term 'scaling form' for a result that has been derived analytically.

tion (1.5) by replacing $p = 1$ with p_c, thus

$$n(s,p) = (p_c - p)^2 \exp(-s/s_\xi), \tag{1.63a}$$

$$s_\xi(p) \propto (p_c - p)^{-1} \qquad \text{for } p \to p_c^-. \tag{1.63b}$$

Clearly, the critical exponent $\sigma = 1$. Apparently, the critical exponent τ must be zero. However, this leads to a contradiction in a relation between the critical exponents τ, σ and γ that we now derive based on the scaling ansatz in Equation (1.62). Following the derivation of the average cluster size in Equation (1.47) and invoking Equation (1.56), we have

$$\begin{aligned} \chi(p) &= s_\xi^{3-\tau}\, \Gamma(3-\tau) && \text{for } p \to p_c \\ &\propto |p - p_c|^{-(3-\tau)/\sigma} && \text{for } p \to p_c \\ &\propto |p - p_c|^{-\gamma} && \text{for } p \to p_c, \end{aligned} \tag{1.64}$$

implying the relation

$$\gamma = \frac{3-\tau}{\sigma}. \tag{1.65}$$

This relation is consistent for the values of the critical exponents on the Bethe lattice for $z > 2$ and on two-dimensional lattices. We will demonstrate shortly that this relation is general, and does not rely on the explicit form of the scaling ansatz in Equation (1.62). In one dimension, we have proved that $\sigma = 1$, see Equation (1.5), and $\gamma = 1$, see Equation (1.15), implying that $\tau = 2$. Assuming that the relation in Equation (1.65) is general, we attempt to rewrite the one-dimensional result for the cluster number density to be consistent with $\tau = 2$ rather than $\tau = 0$:

$$\begin{aligned} n(s,p) &= (p_c - p)^2 \exp(-s/s_\xi) \\ &= s^{-2}[s(p_c - p)]^2 \exp(-s/s_\xi) \\ &= s^{-2}(s/s_\xi)^2 \exp(-s/s_\xi) && \text{for } p \to p_c^- \\ &= s^{-2}\mathcal{G}_{1d}(s/s_\xi) && \text{for } p \to p_c^-, \end{aligned} \tag{1.66}$$

where we have identified $(p_c - p)$ with $1/s_\xi$, which is valid when $p \to p_c^-$, and defined the function

$$\mathcal{G}_{1d}(s/s_\xi) = (s/s_\xi)^2 \exp(-s/s_\xi), \tag{1.67}$$

where the argument is a rescaled cluster size. Thus we can satisfy the relation in Equation (1.65) since we can now identify $\tau = 2$. However, the expression for the cluster number density does not have a pure exponential

decay as a function of s/s_ξ, but a quadratic term in s/s_ξ multiplied by an exponential decay. We therefore propose a yet more general scaling ansatz for the cluster number density, replacing the exponential decay with a general scaling function $\mathcal{G}(s/s_\xi)$ that also includes the one-dimensional result, that is,

$$n(s,p) \propto s^{-\tau}\mathcal{G}(s/s_\xi) \quad \text{for } p \to p_c, s \gg 1, \tag{1.68a}$$

$$s_\xi(p) \propto |p - p_c|^{-1/\sigma} \quad \text{for } p \to p_c, \tag{1.68b}$$

where the characteristic cluster size diverges like a power law in terms of the distance of p from p_c. The function $\mathcal{G}$ is known as the scaling function for the cluster number density.[2]

1.5.1 *Scaling function and data collapse*

An examination of the scaling ansatz for the cluster number density in Equation (1.68) reveals that the p-dependence of the cluster number density on the left-hand side has been taken up by the characteristic cluster size, $s_\xi(p)$, on the right-hand side. A given occupation probability p determines the typical size of the largest cluster. Clusters with size larger than this are extremely rare. Thus we would expect the scaling function $\mathcal{G}(s/s_\xi)$ to decay rapidly for large arguments $s/s_\xi \gg 1$. Note that at $p = p_c$, the characteristic cluster size is infinite, so that $n(s,p_c) \propto s^{-\tau}\mathcal{G}(0)$. Apart from in one dimension, $\mathcal{G}(0)$ is a non-zero constant, therefore at $p = p_c$, the cluster number density decays like a power law for $s \gg 1$. Assuming that the scaling function is well behaved for small arguments, we can Taylor expand it around zero,

$$\mathcal{G}(s/s_\xi) = \mathcal{G}(0) + \mathcal{G}'(0)\,(s/s_\xi) + \frac{1}{2}\mathcal{G}''(0)\,(s/s_\xi)^2 + \cdots . \tag{1.69}$$

In one dimension, $\mathcal{G}_{1d}(0) = \mathcal{G}'_{1d}(0) = 0$ and $\mathcal{G}''_{1d}(0) = 2$ from Equation (1.67). In higher dimensions, however, $\mathcal{G}(0)$ is non-zero. Therefore, the leading order behaviour of the scaling function for $s/s_\xi \ll 1$:

$$\mathcal{G}(s/s_\xi) = \begin{cases} (s/s_\xi)^2 & \text{for } d = 1 \\ \mathcal{G}(0) & \text{for } d > 1. \end{cases} \tag{1.70}$$

[2]Strictly speaking, not one but two scaling functions must be defined, $\mathcal{G}_\pm$, corresponding to $p > p_c$ and $p < p_c$ respectively. We do not discuss the technical reasons for this here, but refer the reader to Appendix C.

For small arguments, the scaling function is quadratic when $d = 1$ and constant when $d > 1$.

Explicitly, the scaling function in Equation (1.68a)

$$\mathcal{G}(s/s_\xi) \propto s^\tau n(s,p) \quad s \gg 1. \tag{1.71}$$

Although the right-hand side of Equation (1.71) is a function of two variables, s and p, or, s and $s_\xi(p)$, the left-hand side is only a function of one variable s/s_ξ, the relative cluster size. Therefore, the cluster number densities are described by a single function, when suitably transformed and viewed in the appropriate relative scale. For cluster sizes, the only relevant scale is the characteristic cluster size.

Assuming that we have a set $\{n(s,p_1), n(s,p_2), n(s,p_3), \ldots\}$ of cluster number densities as a function of s for occupation probabilities $p_1, p_2, p_3, \ldots$, the transformation and rescaling for the cluster number densities is performed in the following way:

(1) For all arguments s, multiply each cluster number density by s^τ to obtain $\{s^\tau n(s,p_1), s^\tau n(s,p_2), s^\tau n(s,p_3) \ldots\}$ as a function of s.
(2) For each transformed cluster number density $s^\tau n(s,p)$, rescale s to s/s_ξ, to obtain $s^\tau n(s,p)$ versus s/s_ξ.

According to Equation (1.71), all the cluster number densities should fall onto the same curve representing the graph of the scaling function $\mathcal{G}$. Such a procedure is known as a data collapse. We now attempt a data collapse for the one-dimensional lattice, the Bethe lattice and two-dimensional lattice, thereby exposing the graphs for the scaling functions $\mathcal{G}_{1d}, \mathcal{G}_{\text{Bethe}}, \mathcal{G}_{2d}$, respectively. Each example will provide some insight into the procedure of data collapse.

1.5.2 *Scaling function and data collapse in $d = 1$*

We take as our set of cluster number densities the graphs in Figure 1.4 with occupation probabilities $p = 0.4, 0.905, 0.99, 0.999, 0.9999$. By studying Figure 1.4, it is plausible that one operation on each degree of freedom should be performed to shift the graphs on top of each other. The first operation in the described procedure transforms each graph in the y-direction in a non-uniform manner by multiplying the cluster number density by s^τ. Figure 1.19(a) displays the transformed set, having multiplied each cluster number density by s^τ for all arguments s, where $\tau = 2$. The distinctive feature of each graph, namely the onset of the rapid decay, now all lie at

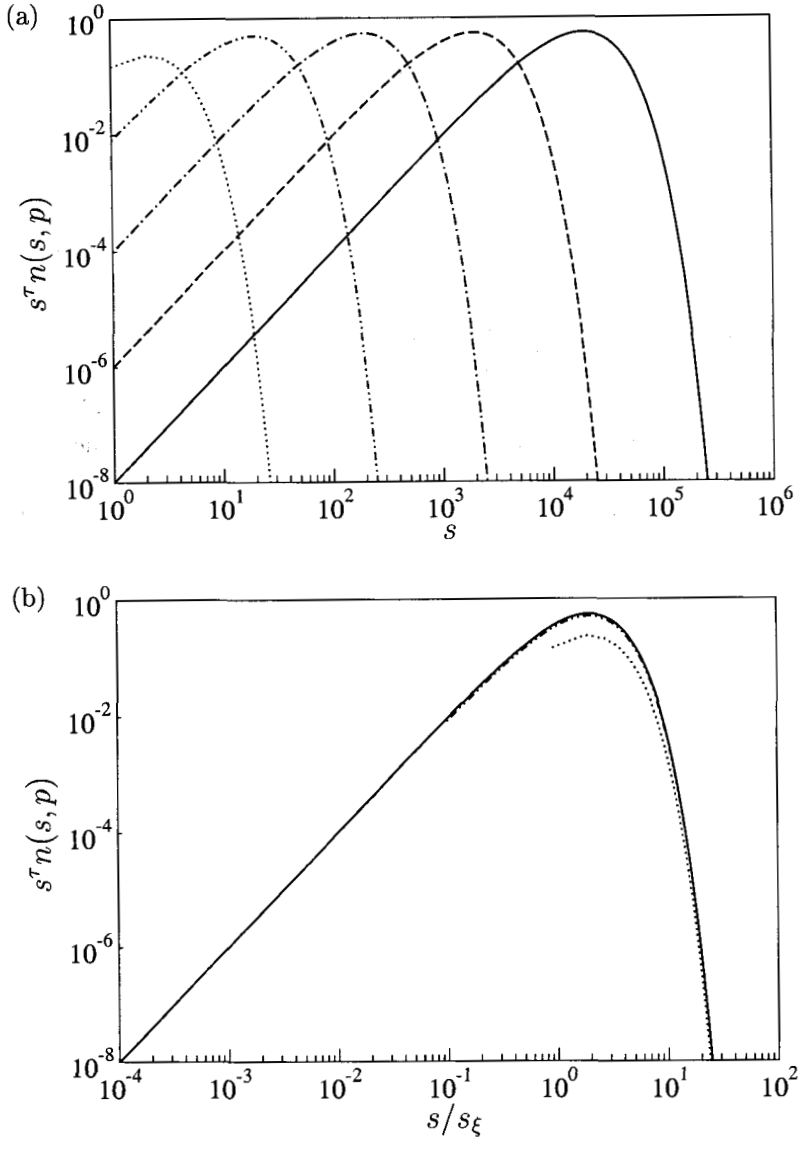

Fig. 1.19 Data collapse of the exact solution of the cluster number densities for one-dimensional percolation for $p = 0.4, 0.905, 0.99, 0.999, 0.9999$. (a) The transformed cluster number density, $s^\tau n(s,p)$, versus the cluster size, s, using the critical exponent $\tau = 2$. (b) The transformed cluster number density, $s^\tau n(s,p)$, versus the rescaled argument, s/s_ξ, where the characteristic cluster size $s_\xi(p) = -1/\ln p$. For $p \to p_c^-$, the curves collapse onto the graph for the scaling function $\mathcal{G}_{1d}(s/s_\xi) = (s/s_\xi)^2 \exp(-s/s_\xi)$.

the same vertical position with only the horizontal position of this feature, given by the characteristic cluster size, distinguishing the graphs.

Thus, to make the graphs in Figure 1.19(a) collapse, we must rescale each argument by $s_\xi(p)$. Figure 1.19(b) displays the transformed and rescaled set, $s^\tau n(s,p)$ versus s/s_ξ. All graphs collapse onto one well-defined function, the scaling function

$$\mathcal{G}_{1\mathrm{d}}\left(s/s_\xi\right) = \left(s/s_\xi\right)^2 \exp(-s/s_\xi). \tag{1.72}$$

For $s/s_\xi \ll 1$, the function grows quadratically, and for $s/s_\xi \gg 1$ it decays rapidly. The crossover between these two behaviours is marked by $s/s_\xi \approx 1$.

The quality of the collapse improves with proximity to the critical point p_c. A scrutinising eye can detect that the graphs corresponding to $p = 0.4, 0.905$ deviate from the collapse. The deviation can be traced to the approximation of $(p_c - p)$ to $1/s_\xi$ in the derivation leading up to Equation (1.66). The validity of this approximation is visualised in Figure 1.5(b). For $p = 0.4$, the approximation is highly dubious, while for $p = 0.905$, the approximation is only slight.

1.5.3 *Scaling function and data collapse on the Bethe lattice*

We take as our set of cluster number densities the graphs in Figure 1.13(b) with occupation probabilities $p = 0.35, 0.45, 0.4842, 0.495$. We do not include the graph in Figure 1.13(a) corresponding to $p = p_c$, since in this case the characteristic cluster size is infinite, making the second operation in the data collapse meaningless.

The relative change in the cluster number density for the Bethe lattice is given by Equation (1.40). Figure 1.20(a) displays the relative change in the cluster number density multiplied by a p-dependent prefactor, versus the cluster size s. The onsets of the rapid decays all lie at the same vertical position, with only the horizontal positions of the onsets, given by the characteristic cluster sizes, distinguishing the graphs.

Accordingly, we rescale each argument by $s_\xi(p)$, see Figure 1.20(b), and obtain a perfect data collapse for all s and p onto the the scaling function

$$\mathcal{G}_{\mathrm{Bethe}}\left(s/s_\xi\right) = \exp\left(-s/s_\xi\right). \tag{1.73}$$

For $s/s_\xi \ll 1$, the scaling function is approximately constant, and for $s/s_\xi \gg 1$ it decays rapidly. The crossover between these two behaviours is marked by $s/s_\xi \approx 1$.

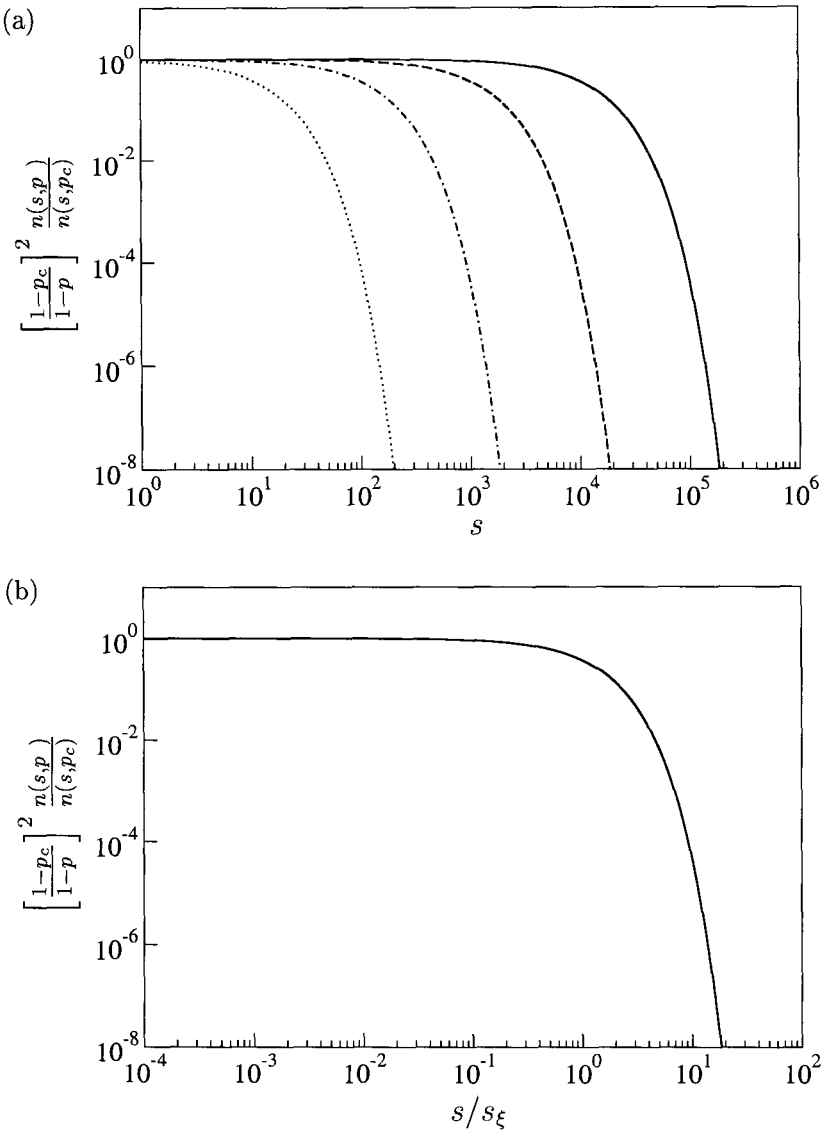

Fig. 1.20 Data collapse of the exact solution of the cluster number densities for percolation on the Bethe lattice for $p = 0.35, 0.45, 0.4842, 0.495$. (a) The relative change in cluster number densities, $[(1-p_c)/(1-p)]^2\, n(s,p)/n(s,p_c)$, versus the cluster size, s. (b) The relative cluster number density, $[(1-p_c)/(1-p)]^2\, n(s,p)/n(s,p_c)$, versus the rescaled argument, s/s_ξ, where the characteristic cluster size, $s_\xi(p) = -1/\ln(4p-4p^2)$. The curves collapse onto the graph for the scaling function $\mathcal{G}_{\text{Bethe}}(s/s_\xi) = \exp\left(-s/s_\xi\right)$.

Only in special cases do we have the exact solution of the cluster number density at $p = p_c$ allowing us to calculate the relative change in the cluster number density applied in the data collapse procedure displayed in Figure 1.20. However, we have argued on general grounds that $n(s, p_c) \propto s^{-\tau}$ for $s \gg 1$ with exponent $\tau = 5/2$. Figure 1.21(a) displays the transformed cluster number density $s^{\tau} n(s, p)$ multiplied by the p-dependent prefactor, versus the cluster size s. The portions of the curves for $n(s, p)$ that were well approximated by $n(s, p) \propto s^{-\tau}$ are now flat. The onsets of the rapid decays all lie at the same vertical position, with only the horizontal positions of the onsets, given by the characteristic cluster sizes, distinguishing the graphs.

Accordingly, we rescale each argument by $s_\xi(p)$ and obtain the data collapse shown in Figure 1.21(b). When using the exact solution of the cluster number density at $p = p_c$, the data collapse is perfect. However, the approximation $n(s, p_c) \propto s^{-\tau}$ is only valid for large cluster sizes, see Figure 1.13. Although the departure from the decaying power law occurs in the range $1 \leq s \lesssim 30$, upon rescaling with $s_\xi(p)$, the departure from the flat portion will be seen at smaller and smaller arguments s/s_ξ as p approaches p_c. Therefore, the curves do not collapse onto $\mathcal{G}_{\text{Bethe}}$ for small cluster sizes. For $s \gtrsim 30$, the collapse is perfect.

Similarly, only in special cases do we have knowledge of the p-dependent prefactor. This factor approaches one as $p \to p_c$ and will therefore not affect the cluster number densities for p close to p_c. Figure 1.22(a) displays the transformed set, having multiplied each cluster number density by s^{τ} for all arguments s, where $\tau = 5/2$. Again, the onsets of the rapid decays all lie at the same vertical position, with only the horizontal positions of the onsets, given by the characteristic cluster sizes, distinguishing the graphs.

After rescaling each argument by $s_\xi(p)$, we obtain the data collapse shown in Figure 1.22(b). The data collapse suffers in the small s behaviour of the cluster number density since the approximation $n(s, p_c) \propto s^{-\tau}$ is only valid in the limit of large cluster sizes. For $s \gtrsim 30$, the collapse is good, particularly for the graphs corresponding to p close to p_c, where the p-dependent prefactor in Equation (1.43a) approaches one.

In summary, for the Bethe lattice, the curves collapse onto the scaling function $\mathcal{G}_{\text{Bethe}} = \exp(-s/s_\xi)$ for $s \gg 1, p \to p_c$. For $s/s_\xi \ll 1$, the scaling function is approximately constant, and for $s/s_\xi \gg 1$ it decays rapidly. The crossover between these two behaviours is marked by $s/s_\xi \approx 1$.

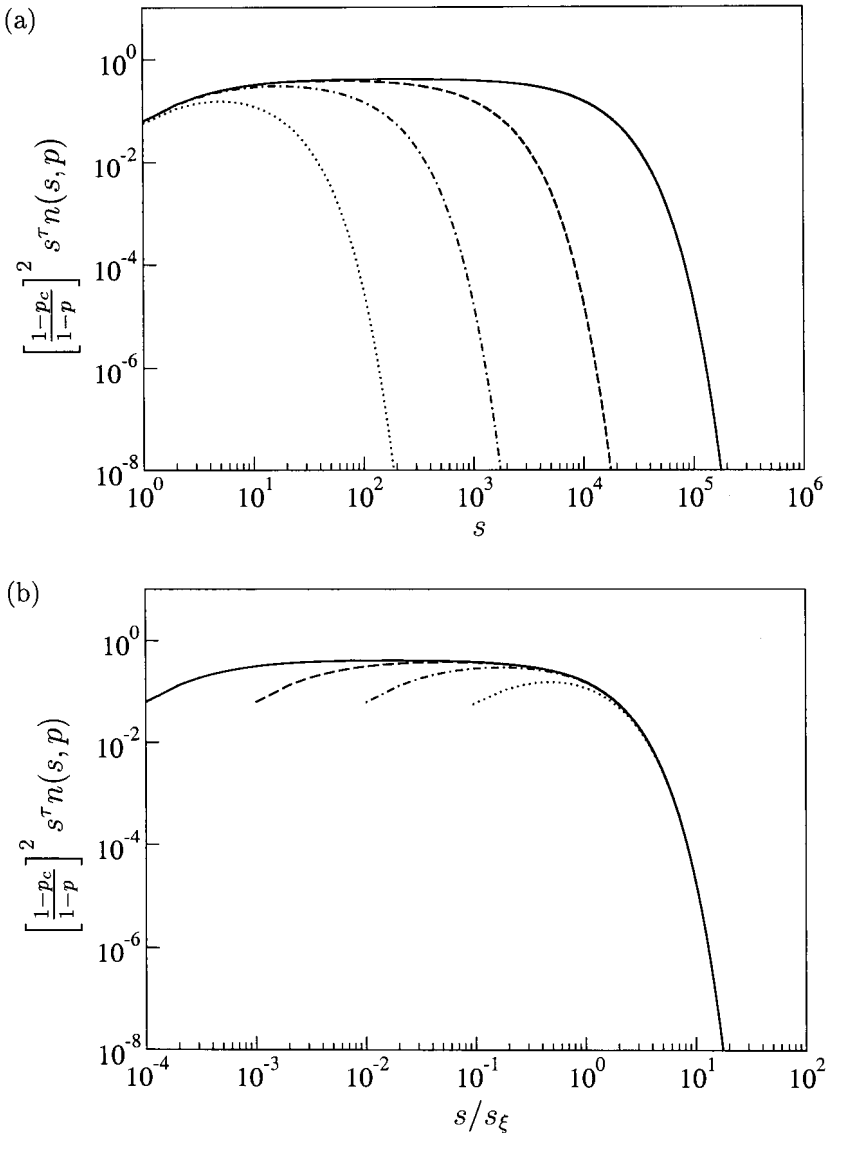

Fig. 1.21 Data collapse of the exact solution of the cluster number densities for percolation on the Bethe lattice for $p = 0.35, 0.45, 0.4842, 0.495$. (a) The transformed cluster number density, $[(1-p_c)/(1-p)]^2\, s^\tau n(s,p)$, versus the cluster size, s, using the critical exponent $\tau = 5/2$. (b) The transformed cluster number density, $[(1-p_c)/(1-p)]^2\, s^\tau n(s,p)$, versus the rescaled argument, s/s_ξ, where the characteristic cluster size, $s_\xi(p) = -1/\ln(4p-4p^2)$. For $s \gg 1$, the curves collapse onto the graph for the scaling function $\mathcal{G}_{\text{Bethe}}(s/s_\xi) = \exp(-s/s_\xi)$.

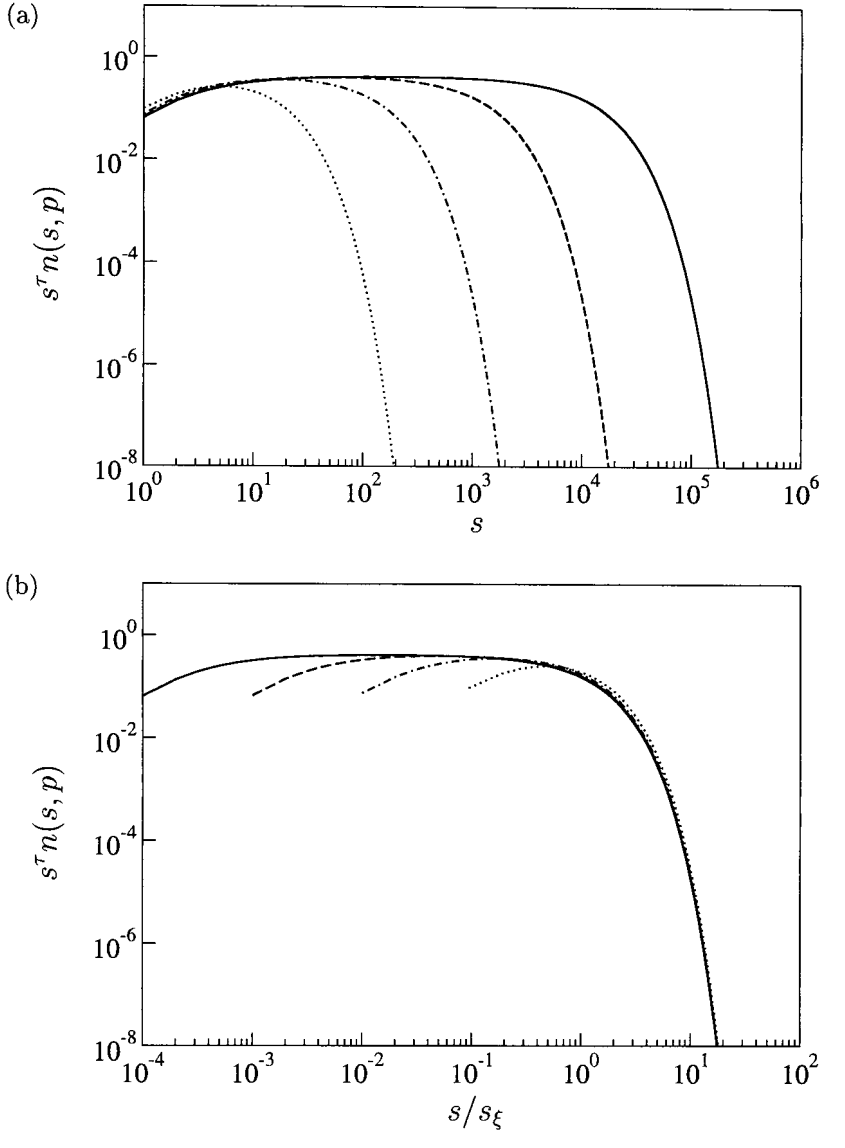

Fig. 1.22 Data collapse of the exact solution of the cluster number densities for percolation on the Bethe lattice for $p = 0.35, 0.45, 0.4842, 0.495$. (a) The transformed cluster number density, $s^\tau n(s,p)$, versus the cluster size, s, using the critical exponent $\tau = 5/2$. (b) The transformed cluster number density, $s^\tau n(s,p)$, versus the rescaled argument, s/s_ξ, where the characteristic cluster size, $s_\xi(p) = -1/\ln(4p - 4p^2)$. For $s \gg 1, p \to p_c$, the curves collapse onto the graph for the scaling function $\mathcal{G}_{\text{Bethe}}(s/s_\xi) = \exp(-s/s_\xi)$.

1.5.4 *Scaling function and data collapse in $d = 2$*

We consider percolation on a two-dimensional square lattice. We take as our set of cluster number densities the graphs in Figure 1.18(a) with occupation probabilities $p = 0.54, 0.55, 0.56, 0.57$ which are approaching the critical occupation probability p_c from below. We do not include the graph in Figure 1.18(b) corresponding to $p = p_c$ for the same reasons as above.

Figure 1.23(a) displays the transformed set, having multiplied each cluster number density by s^τ for all arguments s, where $\tau = 187/91$. The onsets of the rapid decays all lie at the same vertical position, with only the horizontal positions of the onsets, given by the characteristic cluster sizes $s_\xi(p) \propto |p - p_c|^{-1/\sigma}$, distinguishing the graphs.

Accordingly, we rescale each argument by $|p - p_c|^{-1/\sigma}$, using the critical exponent $\sigma = 36/91$. Figure 1.23(b) displays the transformed and rescaled set, $s^\tau n(s,p)$ versus $s|p - p_c|^{1/\sigma}$.

The scaling function $\mathcal{G}_{2\mathrm{d}}$ for the two-dimensional lattice is given by the graph of the data collapse.[3] We have no explicit analytical form for the scaling function. However, for $s/s_\xi \ll 1$, we expect the scaling function to be constant, and for $s/s_\xi \gg 1$ to decay rapidly.

Note that the crossover between these two behaviours in Figure 1.23(b) is apparently displaced from $s/s_\xi = 1$. This is because the argument displayed, $s|p - p_c|^{1/\sigma}$, is only proportional to s/s_ξ and therefore the crossover location is displaced by some unknown factor.

For $s/s_\xi \gtrsim 10^{-2}$ the collapse is good. However, since the approximation $n(s,p_c) \propto s^{-\tau}$ is only valid for large cluster sizes, see Figure 1.18(b), the collapse suffers in the small s behaviour of the cluster number density. Moreover, it appears that the scaling function is not constant for small arguments but increases slightly with s for cluster sizes $1 \ll s \ll s_\xi$. The left-most portion corresponds to the peculiarities of small clusters, while the scaling ansatz only covers cluster sizes $s \gg 1$. Figure 1.18(b) reminds us that the critical exponent $\tau = 187/91$ is defined in the asymptotic limit $s \gg 1$. However, for finite s, there are corrections to the asymptotic behaviour which, in this case, is resulting in an effective (apparent) critical exponent. Therefore, when transforming the cluster number densities, the left-most portions of each graph will increase slightly rather than being constant. We will return to this issue later when discussing finite-size scaling in Section 1.8.

[3] Strictly speaking, since $p \to p_c^-$, the graph of the scaling function outlined in Figure 1.23(b) refers to the branch of $\mathcal{G}_{2\mathrm{d}}$ associated with $p < p_c$.

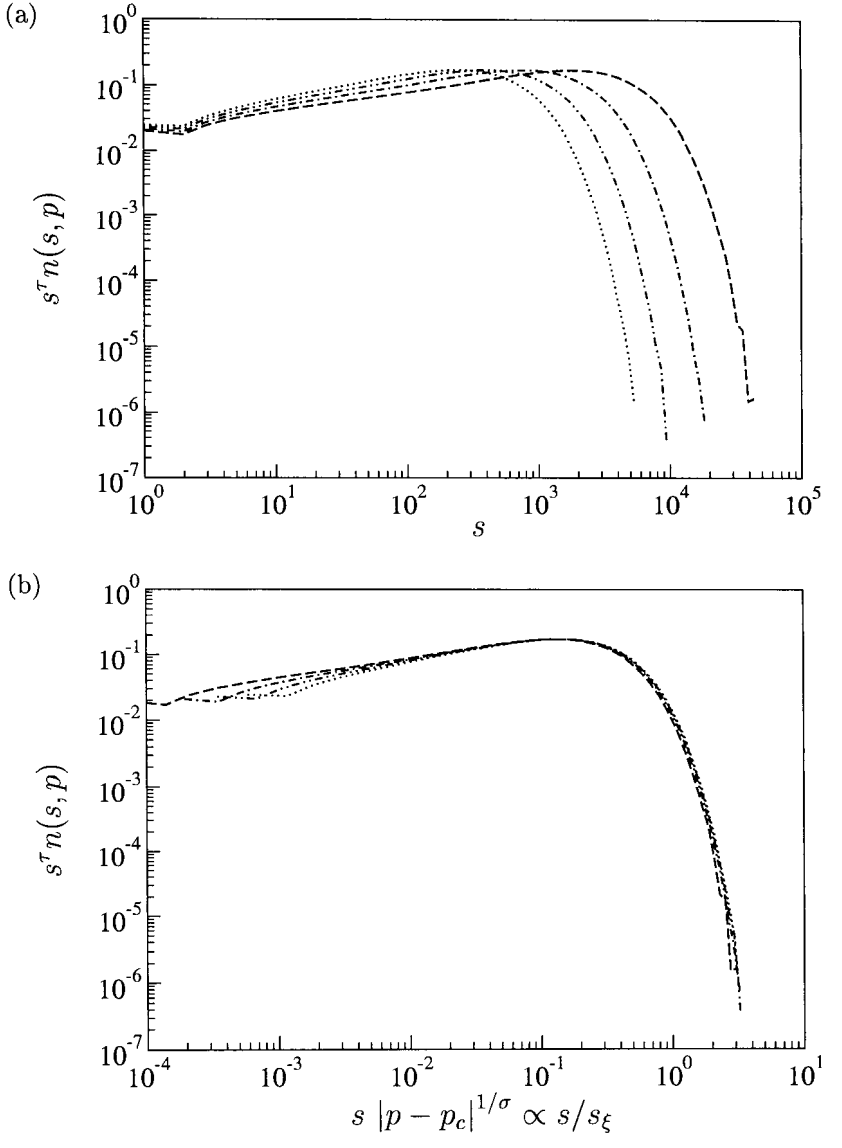

Fig. 1.23 Data collapse of the numerical results for the cluster number densities for two-dimensional site percolation on a square lattice of size $L = 1\,000$ for $p = 0.54, 0.55, 0.56, 0.57$. (a) The transformed cluster number density, $s^\tau n(s,p)$, versus the cluster size, s, using the critical exponent $\tau = 187/91$. (b) The transformed cluster number density, $s^\tau n(s,p)$, versus the rescaled argument, $s\,|p-p_c|^{1/\sigma}$, which is proportional to s/s_ξ, using $\sigma = 36/91$. For $s \gg 1, p \to p_c$, the curves collapse onto the graph for the scaling function $\mathcal{G}_{2d}$.

1.6 Scaling Relations

We have introduced a variety of critical exponents characterising the behaviour of quantities of interest near the critical point. For example, the divergences of the average cluster size $\chi(p)$ and the characteristic cluster size $s_\xi(p)$ are described by the critical exponents γ and σ, respectively. The pick-up of the order parameter $P_\infty(p)$ at $p = p_c$, is described by the critical exponent β. Finally, the critical exponent τ relates the cluster number density $n(s,p)$ to the scaling function $\mathcal{G}(s/s_\xi)$ for $s \gg 1$.

Fortunately, these critical exponents are not independent. We have already derived a relation between the critical exponents γ, τ and σ in Equation (1.65). We will shortly derive an additional relation. Since we will then have two relations for four exponents, once any two exponents are specified, the remaining exponents are fixed. Such constraints among critical exponents are known as scaling relations.

The scaling relation, $\gamma = (3-\tau)/\sigma$, was derived using the prototypical ansatz of the scaling function $\mathcal{G}(x) = \exp(-x)$, see Equation (1.62). We now put the general scaling ansatz for the cluster number density in Equation (1.68) to work by rederiving the above scaling relation.

The average cluster size is proportional to the second moment of the cluster number density. However, for the purpose of making the calculation more general, we will work out the kth moment of the cluster number density, that is,

$$M_k(p) = \sum_{s=1}^{\infty} s^k n(s,p) = \sum_{s=1}^{\infty} s^{k-\tau} \mathcal{G}(s/s_\xi), \tag{1.74}$$

assuming that the general scaling ansatz is valid for all cluster sizes. Replacing the sum by an integral and making the substitution $u = s/s_\xi$, we find

$$\begin{aligned} M_k(p) &\approx \int_1^\infty s^{k-\tau} \mathcal{G}(s/s_\xi)\, ds \\ &= \int_{1/s_\xi}^\infty (us_\xi)^{k-\tau} \mathcal{G}(u) s_\xi \, du \qquad \text{with } u = s/s_\xi \\ &= s_\xi^{1+k-\tau} \int_{1/s_\xi}^\infty u^{k-\tau} \mathcal{G}(u)\, du \\ &\to s_\xi^{1+k-\tau} \int_0^\infty u^{k-\tau} \mathcal{G}(u)\, du \quad \text{for } p \to p_c. \end{aligned} \tag{1.75}$$

Letting p tend to p_c, the characteristic cluster size $s_\xi(p)$ diverges and the lower limit of the integral tends to zero. We will now determine when the definite integral converges. For dimensions $d > 1$, the scaling function is a non-zero constant for small arguments. In this case, for the integral to converge in the lower limit, we must impose the restriction $1 + k - \tau > 0$. For $d = 1$, the scaling function is proportional to u^2 for small arguments. The corresponding restriction $3 + k - \tau > 0$ is satisfied for $k \geq 0$, because in one dimension $\tau = 2$. In the upper limit, the scaling function falls off rapidly for $u \gg 1$, ensuring the convergence of the integral. Since the characteristic cluster size diverges, the contribution from small clusters is suppressed, thus the initial assumption that the general scaling ansatz for the cluster number density is valid for all cluster sizes is not crucial. The definite integral is just a number and thus the kth moment of the cluster number density

$$\begin{aligned} M_k(p) &\propto s_\xi^{1+k-\tau} && \text{for } p \to p_c \\ &\propto |p - p_c|^{-(1+k-\tau)/\sigma} && \text{for } p \to p_c, \end{aligned} \tag{1.76}$$

with the restriction $1 + k - \tau > 0$ for $d > 1$ and $k \geq 0$ for $d = 1$. The second moment corresponds to $k = 2$, and therefore we have rederived the scaling relation

$$\gamma = \frac{3 - \tau}{\sigma}, \tag{1.77}$$

without assuming an explicit form for the scaling function $\mathcal{G}$. In one dimension, $\gamma = 1, \tau = 2, \sigma = 1$. In the Bethe lattice, $\gamma = 1, \tau = 5/2, \sigma = 1/2$. In two dimensions, $\gamma = 43/18, \tau = 187/91$, therefore $\sigma = 36/91$.

Equation (1.76) shows that it is not necessary to introduce new critical exponents for higher moments, because the separation between successive critical exponents is a constant.

An additional scaling relation results from considering the pick-up of the order parameter $P_\infty(p)$ for p approaching p_c from above. This is related to the first moment of the cluster number density by

$$P_\infty(p) = p - \sum_{s=1}^{\infty} s n(s, p), \tag{1.78}$$

as we have already seen in Equation (1.17). To investigate the behaviour of $P_\infty(p)$ as $p \to p_c^+$, we focus on the vicinity of $p = p_c + (p - p_c)$ above p_c.

This is not possible in one dimension. In higher dimensions, however,

$$\begin{aligned} P_\infty(p) &= p - \sum_{s=1}^{\infty} sn(s,p) \\ &= p_c - \sum_{s=1}^{\infty} sn(s,p) + (p - p_c) \\ &= \sum_{s=1}^{\infty} sn(s,p_c) - \sum_{s=1}^{\infty} sn(s,p) + (p - p_c), \end{aligned} \tag{1.79}$$

where we have replaced p_c with just $\sum_{s=1}^{\infty} sn(s,p_c)$ since the order parameter $P_\infty(p_c) = 0$. Combining the sums and assuming once again that the general scaling ansatz for the cluster number density is valid for all s,

$$\begin{aligned} P_\infty(p) &= \sum_{s=1}^{\infty} [sn(s,p_c) - sn(s,p)] + (p - p_c) \\ &\propto \sum_{s=1}^{\infty} s^{1-\tau} [\mathcal{G}(0) - \mathcal{G}(s/s_\xi)] + (p - p_c). \end{aligned} \tag{1.80}$$

Replacing the sum with an integral and making the substitution $u = s/s_\xi$ to reveal the scaling of the order parameter with $s_\xi(p)$, we find

$$\begin{aligned} P_\infty(p) &\propto \int_1^{\infty} s^{1-\tau} [\mathcal{G}(0) - \mathcal{G}(s/s_\xi)]\, ds + (p - p_c) \\ &\propto \int_{1/s_\xi}^{\infty} (us_\xi)^{1-\tau} [\mathcal{G}(0) - \mathcal{G}(u)] s_\xi\, du + (p - p_c) \quad \text{with } u = s/s_\xi \\ &\propto s_\xi^{2-\tau} \int_{1/s_\xi}^{\infty} u^{1-\tau} [\mathcal{G}(0) - \mathcal{G}(u)]\, du + (p - p_c) \\ &\propto s_\xi^{2-\tau} \int_0^{\infty} u^{1-\tau} [\mathcal{G}(0) - \mathcal{G}(u)]\, du + (p - p_c) \qquad \text{for } p \to p_c^+, \end{aligned} \tag{1.81}$$

because the lower limit of the integral tends to zero as p approaches p_c from above. To argue that the definite integral converges, we consider the lower and upper limit separately. For small arguments, $u \ll 1$, we Taylor expand the scaling function $\mathcal{G}(u) = \mathcal{G}(0) + \mathcal{G}'(0)u + \cdots$ to first order. Thus the integrand becomes $u^{2-\tau}\mathcal{G}'(0)$, so that the integral converges in the lower limit for $3 - \tau > 0$, in other words, $\tau < 3$. For large arguments, $u \gg 1$, the scaling function decays rapidly, thus the integrand becomes $u^{1-\tau}\mathcal{G}(0)$. Therefore the integral also converges in the upper limit for $2 - \tau < 0$, in other words, $\tau > 2$.

The pick-up of the order parameter approaching p_c from above is thus

$$P_\infty(p) \propto s_\xi^{2-\tau} \int_0^\infty u^{1-\tau}[\mathcal{G}(0) - \mathcal{G}(u)]\, du + (p - p_c) \qquad \text{for } p \to p_c^+$$

$$\propto (p - p_c)^{(\tau-2)/\sigma} \int_0^\infty u^{1-\tau}[\mathcal{G}(0) - \mathcal{G}(u)]\, du + (p - p_c) \quad \text{for } p \to p_c^+.$$

There are two terms in $(p-p_c)$ with exponents $(\tau-2)/\sigma$ and 1, respectively. Since $(p - p_c)$ tends to zero, the dominating term will have the smaller of the two exponents. It is generally found that $(\tau - 2)/\sigma \leq 1$. Therefore,

$$P_\infty(p) \propto (p - p_c)^{(\tau-2)/\sigma} \propto (p - p_c)^\beta \quad \text{for } p \to p_c^+, \tag{1.82}$$

implying the scaling relation

$$\beta = \frac{\tau - 2}{\sigma}. \tag{1.83}$$

On the Bethe lattice, $\beta = 1, \tau = 5/2, \sigma = 1/2$ and in two dimensions, $\beta = 5/36, \tau = 187/91, \sigma = 36/91$. Although the above derivation is not applicable to one dimension, substituting the values of the critical exponents $\tau = 2, \sigma = 1$ regardless, implies that $\beta = 0$, which is nevertheless consistent, because $P_\infty(p) = (p - p_c)^0 = 1$ at $p = p_c$, see Figure 1.24. The scaling relation in Equation (1.83) is thus valid for all dimensions.

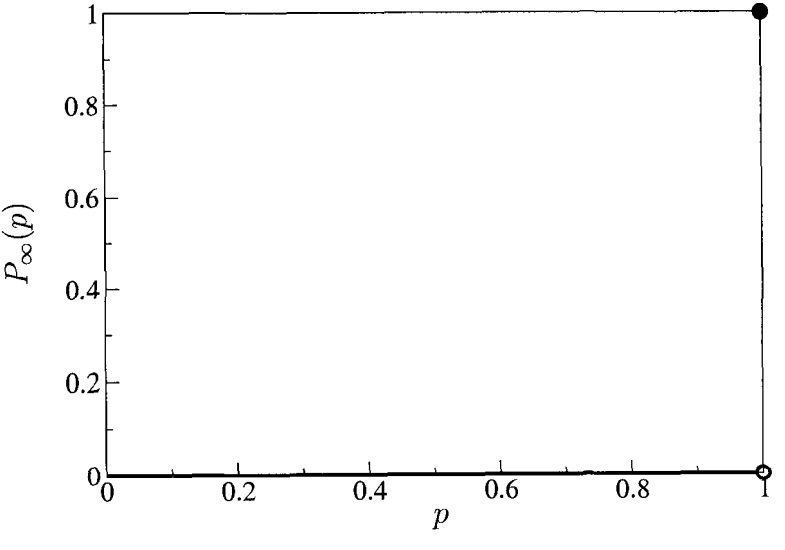

Fig. 1.24 Exact solution of the order parameter, $P_\infty(p)$, versus the occupation probability, p, for one-dimensional percolation. For $p < 1, P_\infty(p) = 0$ while at $p = 1, P_\infty(1) = 1$.

1.7 Geometric Properties of Clusters

At the outset, we asked whether the percolating cluster is a fractal. The cluster number density relates only to the statistics of cluster sizes, but holds no direct information about the geometric properties of clusters. We therefore introduce new quantities and ideas that are, in fact, widely applicable beyond percolation. In doing so, we will indeed show that the incipient infinite cluster is a fractal as the panel corresponding to $p = p_c$ in Figure 1.2 suggests. However, for $p > p_c$, there is a crossover from a fractal percolating cluster on length scales much smaller than a characteristic length scale to a uniform percolating cluster on length scales much larger that the characteristic length scale as the panels corresponding to $p > p_c$ in Figure 1.2 suggest.

1.7.1 *Self-similarity and fractal dimension*

By definition, $P_\infty(p)$ is the probability that a site belongs to the percolating cluster. Up until now, we have focused on the order parameter $P_\infty(p)$ as the quantity that signals the transition from the non-percolating phase with $P_\infty(p) = 0$ for $p \leq p_c$ into the percolating phase above p_c with $P_\infty(p) > 0$. For $p > p_c$, there exists a unique percolating cluster. At $p = p_c$, we will allow ourselves to refer to $P_\infty(p_c)$ as the density of the percolating cluster, even though, strictly speaking, only incipient infinite clusters exist. The following discussion therefore applies to $p \geq p_c$. In one dimension we cannot approach p_c from above, but for completeness we will comment on the trivial case of $d = 1$ when it requires special considerations.

Consider a percolating cluster in an infinite lattice, from which we mark out windows of size ℓ measured in units of the lattice spacing, see Figure 1.25(a).

Within a given window of size ℓ,

$$P_\infty(p;\ell) = \frac{M_\infty(p;\ell)}{\ell^2}, \tag{1.84}$$

where $M_\infty(p;\ell)$ denotes the number of sites of the percolating cluster in that window. For convenience, we will refer to $M_\infty(p;\ell)$ as the 'mass' of the percolating cluster, although it is a dimensionless number. Accordingly, $P_\infty(p;\ell)$ can be alternatively interpreted as being the density (i.e., the number of sites per unit volume) of the percolating cluster within a window of size ℓ.

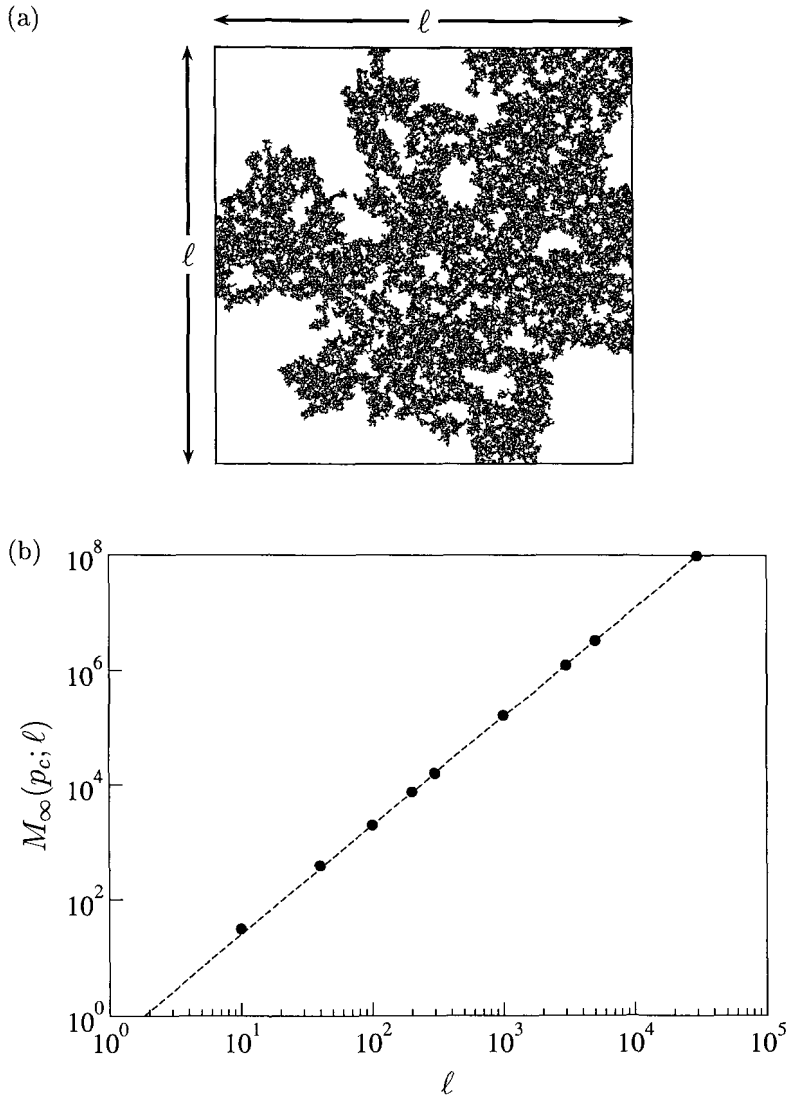

Fig. 1.25 Incipient infinite cluster in two-dimensional site percolation on a square lattice at occupation probability $p = p_c$. (a) Part of an incipient infinite cluster. Qualitatively, the incipient infinite cluster is an irregular, rough-edged structure, perforated by holes of all sizes limited only by the size of the window. The cluster extends into all the available space, however, its density decreases with distance. (b) Numerical results for the mass, $M_\infty(p_c;\ell)$, of an incipient infinite cluster versus the window size, ℓ (solid circles). For large ℓ, the mass increases as a power law in the window size, $M_\infty(p_c;\ell) \propto \ell^D$, where the exponent D is the fractal dimension. The dashed straight line has slope 91/48.

Since, by definition,

$$P_\infty(p) = \lim_{\ell \to \infty} P_\infty(p; \ell), \tag{1.85}$$

the density of the percolating cluster in the infinite lattice is zero at $p = p_c$, except in one dimension where $P_\infty(p_c) = 1$. How are we to reconcile the vanishing density with Equation (1.84)? To answer this, we study the mass of an incipient infinite cluster as a function of window size ℓ, see Figure 1.25(b).

The numerical data are consistent with

$$M_\infty(p_c; \ell) \propto \ell^D, \tag{1.86}$$

where D is known as the fractal dimension of the incipient infinite cluster. In two dimensions, $D = 91/48 \approx 1.90$. The power-law increase in the mass of an incipient infinite cluster with window size ℓ at $p = p_c$ is also seen in higher dimensions but with different fractal dimensions $D < d$, except in one dimension where $D = d = 1$. In the Bethe lattice, $D = 4$. Thus an incipient infinite cluster is indeed a fractal characterised by its fractal dimension D. The density of an incipient infinite cluster

$$P_\infty(p_c; \ell) = \frac{M_\infty(p_c; \ell)}{\ell^2} \propto \ell^{D-d} \tag{1.87}$$

decreases with increasing window size ℓ, for $d > 1$ and by Equation (1.85), $P_\infty(p_c) = 0$, as required.

This implies two unique properties of a fractal that may, at first, appear somewhat counterintuitive. First, the density of a fractal depends on the length scale ℓ on which it is measured. As many objects in Nature are fractal, such knowledge is crucial if one wants to estimate the density of an object on a length scale ℓ_2, based on the density measured on another length scale ℓ_1, see Appendix D. Second, the density of a fractal always decreases with increasing window size ℓ, irrespective of where on the fractal the window is placed.

Just by looking at the fractal in Figure 1.25(a), it would not be easy to conjecture the above properties. However, qualitatively, the decrease in the density of a fractal is caused by the holes inside it. If the holes were limited up to some characteristic size, then for sufficiently large windows, the density of a fractal would no longer decrease but become constant. If, on the other hand, there were no upper limit to the size of the holes, then larger windows would admit successively larger holes, maintaining the decrease in the density of a fractal.

Another important qualitative feature of fractals is self-similarity, which we will quantify later in Section 1.7.4. Figure 1.26 shows two incipient infinite clusters. Figure 1.26(a) (which is a reproduction of the incipient infinite cluster in Figure 1.25(a)) looks similar, at least statistically, to the incipient infinite cluster in Figure 1.26(b). The two incipient infinite clusters apparently have the same window size. However, a reader with keen eyesight will have spotted that the incipient infinite cluster in Figure 1.26(b) is in fact a rescaled version of the upper-right quarter of the incipient infinite cluster in Figure 1.26(a). This is the essence of self-similarity. A self-similar object looks alike on all length scales. For a further discussion of fractals, see Appendix D and for general reviews see [Feder, 1988; Falconer, 2003].

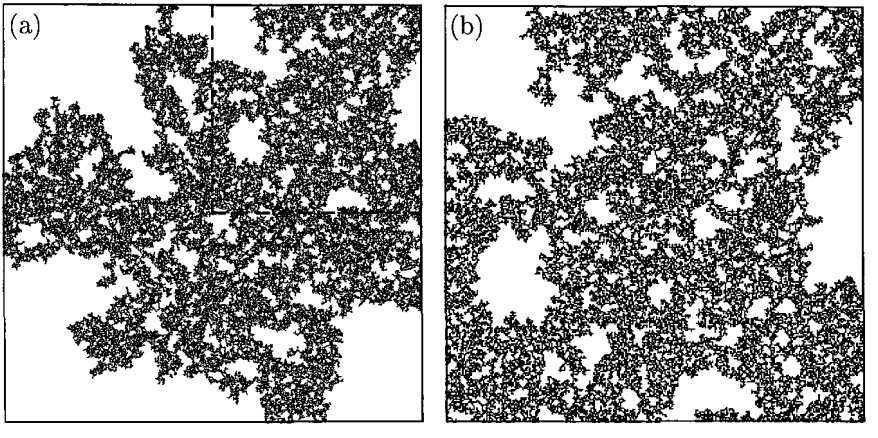

Fig. 1.26 Parts of two incipient infinite clusters in two-dimensional site percolation on a square lattice at occupation probability $p = p_c$. The incipient infinite cluster in (b) is a rescaled version of the upper right quarter of the incipient infinite cluster in (a).

1.7.2 *Mass of a large but finite cluster at $p = p_c$*

The relationship $M_\infty(p_c; \ell) \propto \ell^D$ applies to the mass of an incipient infinite cluster at $p = p_c$. How does the mass $M(s, p_c; \ell)$ of a large but finite cluster $s \gg 1$ behave at $p = p_c$? For small length scales ℓ, we do not know that the cluster we are considering is finite. Thus we would expect to find $M(s, p_c; \ell) \propto \ell^D$ where D is the fractal dimension of the incipient infinite cluster. However, for large length scales, contrary to the incipient infinite cluster, the finite cluster will be fully contained within a window of size ℓ with $M(s, p_c; \ell) = s$, see Figure 1.27.

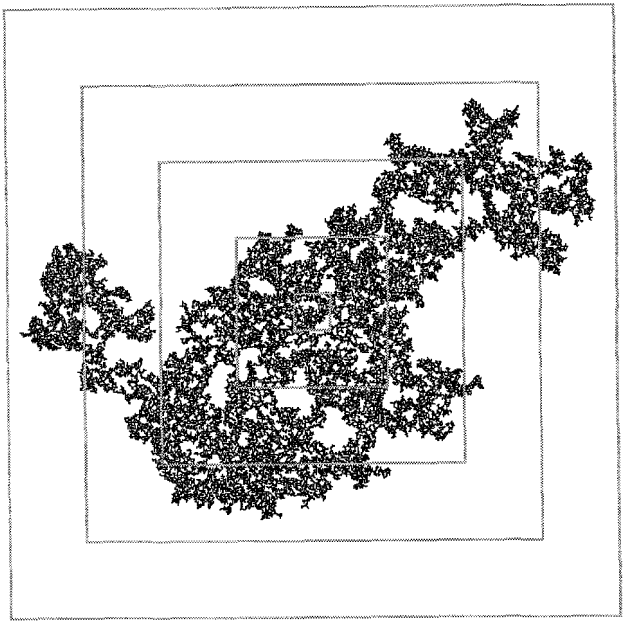

Fig. 1.27 A finite cluster of size $s = 42\,153$ in two-dimensional site percolation on a square lattice at occupation probability $p = p_c$. The origin of the windows is placed in the centre of mass of the s-cluster. For small window sizes, ℓ, the finite cluster appears fractal. When ℓ is large, the finite cluster will be fully contained within the windows, revealing that the cluster is, in fact, finite.

Thus the mass of a large s-cluster at $p = p_c$ satisfies

$$M(s, p_c; \ell) \propto \begin{cases} \ell^D & \text{for small } \ell \\ s & \text{for large } \ell. \end{cases} \tag{1.88}$$

In order to quantify what we mean by 'small' and 'large' ℓ, we define the radius of gyration, R_s, which is a measure of the linear scale of s-clusters in units of the lattice spacing. Assume that the positions of the occupied sites in a given s-cluster are denoted by $\mathbf{r}_i, i = 1, \ldots, s$. The centre of mass of the cluster is defined as

$$\mathbf{r}_{\text{cm}} = \frac{1}{s} \sum_{i=1}^{s} \mathbf{r}_i, \tag{1.89}$$

see Figure 1.28, while its radius of gyration squared is defined as the average

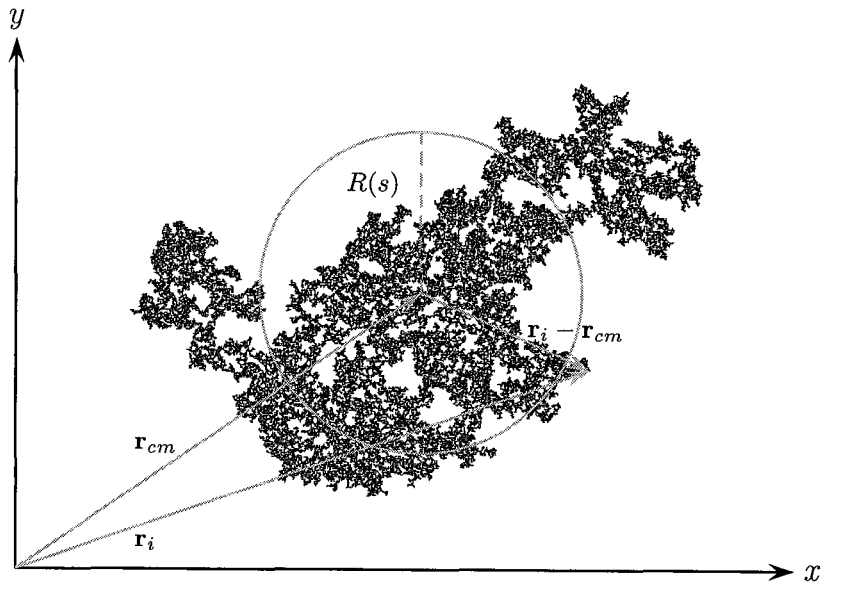

Fig. 1.28 A finite cluster of size $s = 42\,153$ in two-dimensional site percolation on a square lattice. The centre of mass is given by the position $\mathbf{r}_{\rm cm}$, and $|\mathbf{r}_i - \mathbf{r}_{\rm cm}|$ is the distance of occupied site $\mathbf{r}_i$ to the centre of mass $\mathbf{r}_{\rm cm}$. The radius of gyration, $R(s) \approx 153$ in units of the lattice spacing, is a measure of the linear size of the s-cluster (dashed line).

square distance to the centre of mass,

$$R^2(s) = \frac{1}{s}\sum_{i=1}^{s} |\mathbf{r}_i - \mathbf{r}_{\rm cm}|^2. \tag{1.90}$$

We denote by R_s^2 the average of $R^2(s)$ over the ensemble of all clusters of size s. Thus, more precisely,

$$M(s, p_c; \ell) \propto \begin{cases} \ell^D & \text{for } \ell \ll R_s \\ s & \text{for } \ell \gg R_s. \end{cases} \tag{1.91}$$

The average radius of gyration R_s is the sole length scale in the problem. For window sizes $\ell \lesssim R_s$, the cluster appears infinite to all intents and purposes. Therefore we would expect the relation $M(s, p_c; \ell) \propto \ell^D$ to hold all the way up to $\ell \approx R_s$, so that $s \propto R_s^D$. The same result is obtained by imposing continuity of $M(s, p_c; \ell)$ to ensure that the two limiting behaviours match up at $\ell \approx R_s$. From the right-hand side of Equation (1.91) it is

apparent that only the ratio between the two length scales ℓ and R_s is relevant for characterising the behaviour of the mass of a large s-cluster at $p = p_c$ as a function of window size ℓ. We can summarise the crossover from the fractal behaviour for $\ell/R_s \ll 1$ to the trivial behaviour for $\ell/R_s \gg 1$ by introducing a crossover function, see Figure 1.29,

$$m(\ell/R_s) \propto \begin{cases} \text{constant} & \text{for } \ell/R_s \ll 1 \\ (\ell/R_s)^{-D} & \text{for } \ell/R_s \gg 1, \end{cases} \tag{1.92}$$

such that

$$M(s, p_c; \ell) = \ell^D m(\ell/R_s) \propto \begin{cases} \ell^D & \text{for } \ell/R_s \ll 1 \\ R_s^D & \text{for } \ell/R_s \gg 1. \end{cases} \tag{1.93}$$

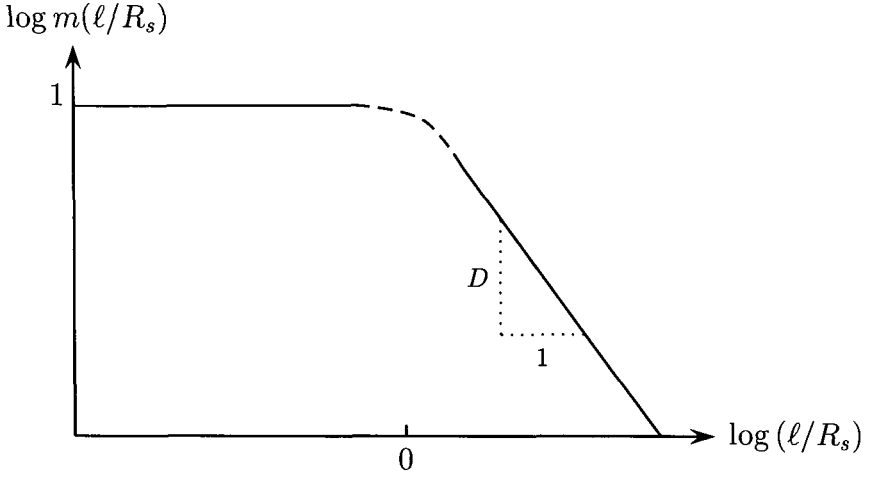

Fig. 1.29 A sketch of the crossover function, $m(\ell/R_s)$, for the mass of a large but finite cluster at $p = p_c$ versus the ratio, ℓ/R_s. The solid lines indicate the limiting behaviour of the crossover function, that is, constant for small arguments and decaying like a power law with exponent $-D$ for large arguments. The dashed line indicates that the crossover function is not known exactly in the region $\ell \approx R_s$.

On small length scales $\ell \ll R_s$, the crossover function is a constant and the cluster appears fractal. On large length scales $\ell \gg R_s$, the crossover function decays as a power law with exponent $-D$ and the cluster is finite with constant mass. The crossover takes place in the region $\ell \approx R_s$, where the exact form of the crossover function is not known.

1.7.3 *Correlation length*

For a particular characteristic cluster size $s_\xi(p)$ fixed by the occupation probability p, the associated radius of gyration defines a characteristic length scale that is proportional to the correlation length;[4] hence, we have

$$s_\xi \propto \xi^D. \tag{1.94}$$

Figure 1.30 is a sketch of the correlation length versus occupation probability. The vertical dotted line shows the position of the critical occupation probability p_c.

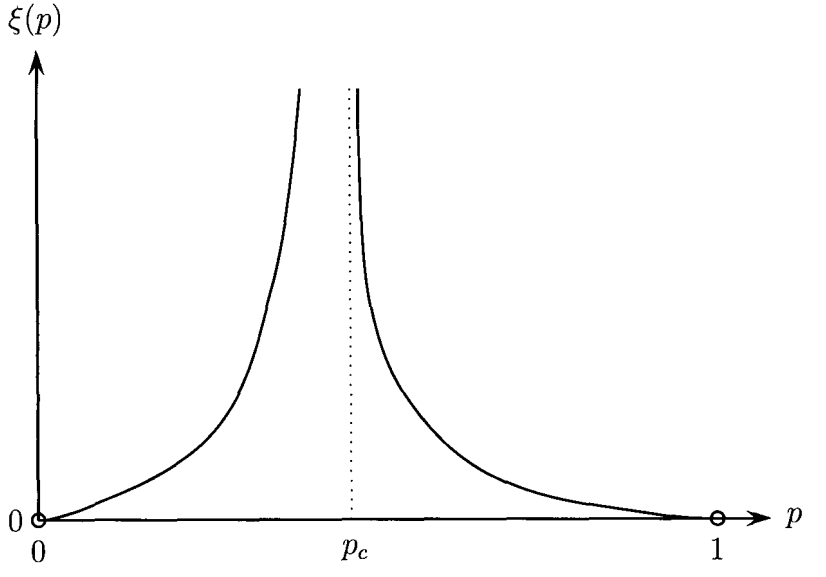

Fig. 1.30 A sketch of the correlation length, $\xi(p)$, versus the occupation probability, p. The vertical dotted line shows the position of p_c. For $p \to p_c$, the correlation length diverges as a power law with exponent $-\nu$ in terms of $|p - p_c|$, the distance of p from p_c, that is, $\xi(p) \propto |p - p_c|^{-\nu}$. For $p \to 0^+$ and $p \to 1^-$, the correlation length tends to zero.

The correlation length is the typical radius of the largest finite cluster, both below and above p_c. Since the correlation length is only defined for finite clusters, the percolating infinite cluster is excluded when $p > p_c$. Also, since finite clusters reside inside the holes of the percolating cluster when $p > p_c$, the correlation length can be identified with the typical radius of the largest holes in the percolating cluster, see Figure 1.2.

[4]For a discussion on the various different characteristic length scales and their interrelationship, see [Stauffer and Aharony, 1994].

Just as the characteristic cluster size diverges for p approaching p_c, so too does the correlation length. Thus at $p = p_c$, since there are finite clusters of all sizes, so too are there holes of all sizes in the incipient infinite cluster. The divergence is characterised by the critical exponent ν, where

$$\xi(p) \propto |p - p_c|^{-\nu} \quad \text{for } p \to p_c. \tag{1.95}$$

In one dimension, $\nu = 1$, see Equation (1.20). In two dimensions, $\nu = 4/3$. In the Bethe lattice, $\nu = 1/2$.

We have now introduced two 'new' critical exponents, the fractal dimension D of the incipient infinite cluster, and the exponent ν, characterising the divergence of the correlation length as p approaches p_c. To keep the number of independent critical exponents down to two, we must derive two additional scaling relations to accommodate D and ν.

The first of these follows immediately from Equation (1.94) and the definitions of the critical exponents σ and ν,

$$\begin{aligned} s_\xi &\propto \xi^D \\ &\propto |p - p_c|^{-D\nu} \quad \text{for } p \to p_c \\ &\propto |p - p_c|^{-1/\sigma} \quad \text{for } p \to p_c, \end{aligned} \tag{1.96}$$

implying the scaling relation

$$D = \frac{1}{\nu\sigma}. \tag{1.97}$$

In one dimension, $D = 1$, $\nu = 1$, and $\sigma = 1$. In two dimensions, $D = 91/48$, $\nu = 4/3$, and $\sigma = 36/91$. In the Bethe lattice, $D = 4$, $\nu = 1/2$, and $\sigma = 1/2$.

1.7.4 *Mass of the percolating cluster for $p > p_c$*

The second scaling relation comes about by considering the mass of the percolating cluster. As we have just seen, it is important to identify the relevant length scale in the problem. In the case of a large but finite cluster at $p = p_c$, where the correlation length $\xi(p)$ is infinite, the only relevant length scale is the average radius of gyration. The mass $M(s, p_c; \ell)$ of the finite cluster within a window of size ℓ therefore depends only on the ratio ℓ/R_s.

In the case of the percolating cluster for $p > p_c$, the only relevant length scale is the correlation length, $\xi(p)$. Thus we are led to consider the two limits, $\ell \ll \xi$ and $\ell \gg \xi$, in order to determine the mass $M_\infty(\xi; \ell)$ of the

percolating cluster within a window of size ℓ at occupation probability p. Since a particular value of p fixes the correlation length, see Figure 1.30, we have replaced the p-dependence of the mass with a $\xi(p)$-dependence in order to make the comparison of length scales explicit.

For sufficiently small window sizes, $\ell \ll \xi$, it is not possible to detect whether the correlation length is finite. The percolating cluster appears fractal with holes of all sizes limited only by ℓ, thus

$$M_\infty(\xi;\ell) \propto \ell^D \quad \text{for } \ell \ll \xi. \tag{1.98}$$

Note that at $p = p_c$, the correlation length is infinite, guaranteeing that $\ell \ll \xi$ for all window sizes ℓ. The incipient infinite cluster is fractal on all length scales. When $p > p_c$, however, the opposite limit is accessible.

For sufficiently large window sizes, $\ell \gg \xi$, the holes are limited in size by $\xi(p)$ and are fully enclosed within the windows.

Given that we know how to calculate the mass of a fractal object, we divide the window into boxes of size $\xi(p)$ such that within each box the percolating cluster is a fractal with mass proportional to ξ^D, see Figure 1.31.

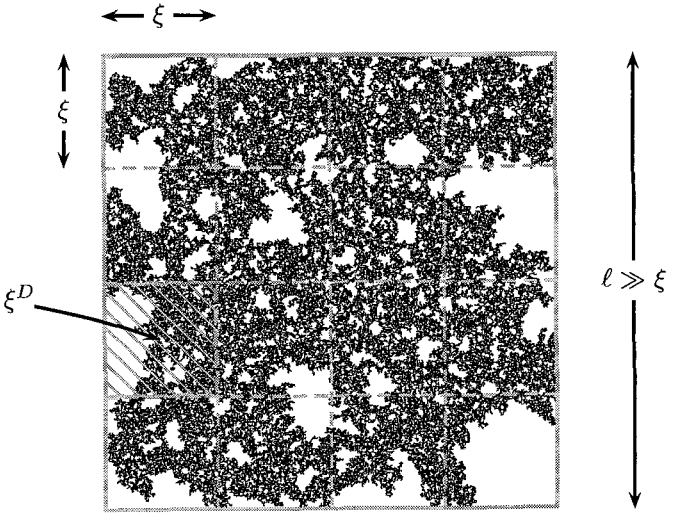

Fig. 1.31 A large window of size $\ell \gg \xi$ containing a percolating cluster at $p > p_c$ subdivided into $(\ell/\xi)^d$ boxes of size $\xi(p)$. On scales up to $\xi(p)$, the percolating cluster is a fractal. Therefore, the mass of the percolating cluster within each box is proportional to ξ^D.

In d-dimensions, the number of such boxes is $(\ell/\xi)^d$, therefore

$$\begin{aligned} M_\infty(\xi;\ell) &\propto (\ell/\xi)^d \xi^D \quad \text{for } \ell \gg \xi \\ &= \xi^{D-d}\ell^d \quad \text{for } \ell \gg \xi. \end{aligned} \tag{1.99}$$

Equation (1.99) is reminiscent of the formula mass = density × volume, identifying ξ^{D-d} as the density of the percolating cluster for length scales $\ell \gg \xi$, and ℓ^d as the volume of the window. Therefore, on scales $\ell \gg \xi$, the percolating cluster looks uniform with density ξ^{D-d}. But we also know that the density of the percolating cluster is simply given by the order parameter, that is,

$$\begin{aligned} M_\infty(\xi;\ell) &= P_\infty(p;\ell)\ell^d \\ &= P_\infty(p)\ell^d \quad \text{for } \ell \gg \xi \\ &\propto (p-p_c)^\beta \ell^d \quad \text{for } \ell \gg \xi, p \to p_c^+ \\ &\propto \xi^{-\beta/\nu}\ell^d \quad \text{for } \ell \gg \xi, p \to p_c^+, \end{aligned} \tag{1.100}$$

where, in the last step, we have exploited the behaviour of the correlation length near p_c. By comparing Equations (1.99) and (1.100), we read off the scaling relation

$$D - d = -\frac{\beta}{\nu}. \tag{1.101}$$

Such a scaling relation which involves the dimensionality d is commonly called a hyperscaling relation. Although the above derivation is not applicable to one dimension because we cannot approach p_c from above, substituting $D = 1$ and $d = 1$ regardless, implies $\beta = 0$, which is nevertheless consistent. In two dimensions, $D = 91/48$, $\beta = 5/36$, and $\nu = 4/3$. In the Bethe lattice, $D = 4$, $\beta = 1$, and $\nu = 1/2$ implies $d = 6$. We will be able to interpret this result shortly.

Collecting together the results for the two limits, the mass of the percolating cluster

$$M_\infty(\xi;\ell) \propto \begin{cases} \ell^D & \text{for } \ell \ll \xi \\ \ell^D(\ell/\xi)^{d-D} & \text{for } \ell \gg \xi, \end{cases} \tag{1.102}$$

where, for $\ell \gg \xi$, the right-hand side of Equation (1.99) has been reorganised.

Just as for a large finite cluster at $p = p_c$, we can summarise these two limiting behaviours by introducing a crossover function,

$$m_\infty(\ell/\xi) \propto \begin{cases} \text{constant} & \text{for } \ell \ll \xi \\ (\ell/\xi)^{d-D} & \text{for } \ell \gg \xi, \end{cases} \tag{1.103}$$

such that

$$M_\infty(\xi;\ell) = \ell^D m_\infty(\ell/\xi). \tag{1.104}$$

Equation (1.104) represents a crossover from fractal behaviour at length scales $\ell \ll \xi$ where the mass increases as ℓ^D, to non-fractal uniform behaviour at length scales $\ell \gg \xi$ where the mass increases as ℓ^d.

At $p = p_c$, the correlation length is infinite and only the fractal behaviour will be observed without any crossover to non-fractal uniform behaviour, that is,

$$M_\infty(\infty;\ell) = \ell^D m_\infty(0). \tag{1.105}$$

The left-hand side of Equation (1.104) is a function of the two length scales while the crossover function on the right-hand side is only a function of the ratio ℓ/ξ of the two length scales.

Since the crossover function, m_∞, is a function of the ratio ℓ/ξ, it is invariant under reduction of length scales $\xi \mapsto \xi/b, \ell \mapsto \ell/b$, where $b > 1$ is a dimensionless scale factor. After rescaling, the mass of the percolating cluster becomes

$$\begin{aligned} M_\infty(\xi/b;\ell/b) &= (\ell/b)^D m_\infty(\ell/\xi) \\ &= b^{-D} M_\infty(\xi;\ell); \end{aligned} \tag{1.106}$$

therefore, the mass of the percolating cluster satisfies

$$M_\infty(\xi;\ell) = b^D M_\infty(\xi/b;\ell/b) \quad \text{for } b > 1. \tag{1.107}$$

A function that obeys Equation (1.107) is known as a homogeneous function, see Appendix C.

We now show that we can recover the limiting forms for the mass of the percolating cluster in Equation (1.102). In doing so, we demonstrate that Equation (1.104), involving the crossover function, and Equation (1.107), expressing the homogeneity of the mass of the percolating cluster, are equivalent.

For both limits $\ell \ll \xi$ and $\ell \gg \xi$, our approach will be similar. We rescale all length scales such that the lesser of ξ and ℓ is equal to unity in

terms of the lattice spacing. The lattice spacing constitutes a lower cutoff, below which it makes no sense to rescale.

Consider the limit $\ell \ll \xi$ and rescale ξ and ℓ by the factor $b = \ell$,

$$M_\infty(\xi;\ell) = \ell^D M_\infty(\xi/\ell;1) \propto \ell^D \quad \text{for } \ell \ll \xi, \tag{1.108}$$

because the mass $M_\infty(\xi/\ell, 1)$ within a window of unit size and correlation length $\xi/\ell \gg 1$ is constant.

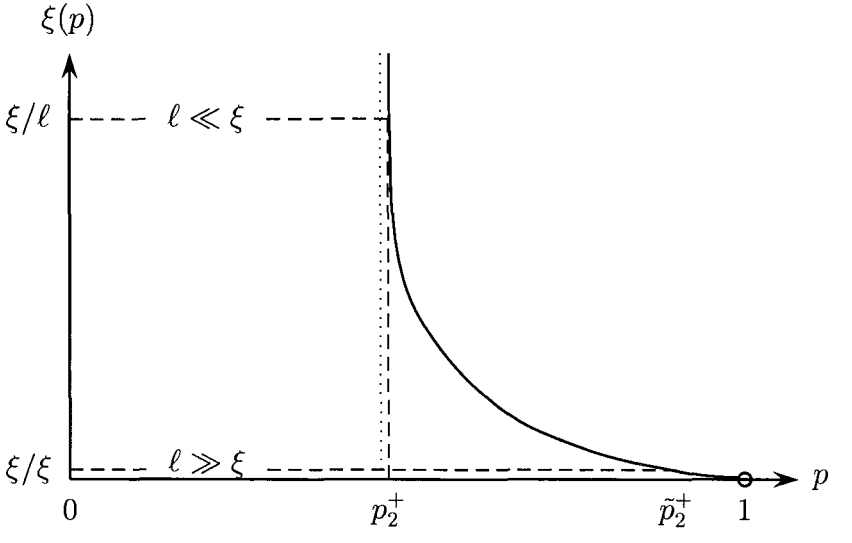

Fig. 1.32 A sketch of the correlation length, ξ, versus the occupation probabilities $p > p_c$. The vertical dotted line shows the position of p_c. For $p \to p_c^+$, the correlation length diverges as a power law with exponent $-\nu$ in terms of $(p - p_c)$, the distance of p above p_c, that is, $\xi(p) \propto (p - p_c)^{-\nu}$. For $p \to 1^-$, the correlation length tends to zero.

To justify that $M_\infty(\xi/\ell, 1)$ is a constant in the limit $\xi/\ell \gg 1$, we appeal to Figure 1.32, which is a sketch of the correlation length versus occupation probability for $p > p_c$. A particular value of p fixes the correlation length and vice versa. At $p = p_c$, the correlation length is infinite and holes of all sizes exist. For $p > p_c$ the correlation length is finite, so that there is a largest typical size of holes. With increasing p, the percolating cluster occupies more and more space. As the holes in the percolating cluster shrink, the correlation length decreases. For p approaching one, the largest typical size of a hole approaches one. At $p = 1$, there are no holes left, and the correlation length is zero.

At $p = p_c$, where ξ is infinite, and at $p = 1$, where ξ is zero, the correlation length remains invariant upon rescaling. However, reducing a finite correlation length by a factor $b > 1$, $\xi \mapsto \xi/b$, effectively corresponds to increasing the occupation probability p.

Consider an initial correlation length set by an initial occupation probability p_1^+ slightly above p_c, and $\ell \ll \xi$. Upon rescaling by the factor $b = \ell$, the correlation length reduces to ξ/ℓ, while the effective occupation probability increases slightly to p_2^+, as shown in Figure 1.32. Thus the mass $M_\infty(\xi/\ell, 1)$ within a window of unit size and correlation length $\xi/\ell \gg 1$ is the probability p_2^+ of occupying a single site.

Now, consider the limit $\ell \gg \xi$ and rescale ξ and ℓ by the factor $b = \xi$,

$$\begin{aligned} M_\infty(\xi; \ell) &= \xi^D M_\infty(1; \ell/\xi) \\ &\propto \xi^{D-d} \ell^d \qquad \text{for } \ell \gg \xi \end{aligned} \tag{1.109}$$

because the mass $M_\infty(1, \ell/\xi)$ within a window of size ℓ/ξ and unit correlation length equals the volume of the window $(\ell/\xi)^d$.

Consider once again an initial correlation length set by an initial occupation probability $\tilde{p}_1^+$ slightly above p_c, and $\ell \gg \xi$. Upon rescaling by the factor $b = \xi$, the correlation length reduces to 1, while the effective occupation probability increases markedly to $\tilde{p}_2^+ \approx 1$, as shown in Figure 1.32. Thus the mass $M_\infty(1, \ell/\xi)$ within a window of size ℓ/ξ and unit length is the probability $\tilde{p}_2^+ \approx 1$ of occupying a single site multiplied by the number of sites $(\ell/\xi)^d$.

By identification,

$$\begin{aligned} M_\infty(\xi; \ell) &= \ell^D m_\infty(\ell/\xi) \\ &= \begin{cases} \ell^D M_\infty(\xi/\ell; 1) & \text{for } \ell \ll \xi \\ \xi^D M_\infty(1; \ell/\xi) & \text{for } \ell \gg \xi. \end{cases} \end{aligned} \tag{1.110}$$

The limiting behaviours of the crossover function given in Equation (1.103) is therefore related to the mass of the percolating cluster in the manner

$$m_\infty(\ell/\xi) = \begin{cases} M_\infty(\xi/\ell; 1) & \text{for } \ell \ll \xi \\ (\ell/\xi)^{-D} M_\infty(1; \ell/\xi) & \text{for } \ell \gg \xi, \end{cases} \tag{1.111}$$

where the right-hand side is only a function of the ratio ℓ/ξ.

It is also informative to examine the density of the percolating cluster

in the two limits with the help of Equation (1.102),

$$P_\infty(\xi;\ell) = \frac{M_\infty(\xi;\ell)}{\ell^d} \propto \begin{cases} \ell^{D-d} & \text{for } \ell \ll \xi \\ \xi^{D-d} & \text{for } \ell \gg \xi; \end{cases} \tag{1.112}$$

see Figure 1.33. The length scale that will determine the density is the lesser of the two length scales ℓ and ξ. The density decreases as ℓ^{D-d} with increasing window size for length scales $\ell \ll \xi$ – the percolating cluster looks fractal. The density remains constant at value ξ^{D-d} for length scales $\ell \gg \xi$ – the percolating cluster looks uniform.

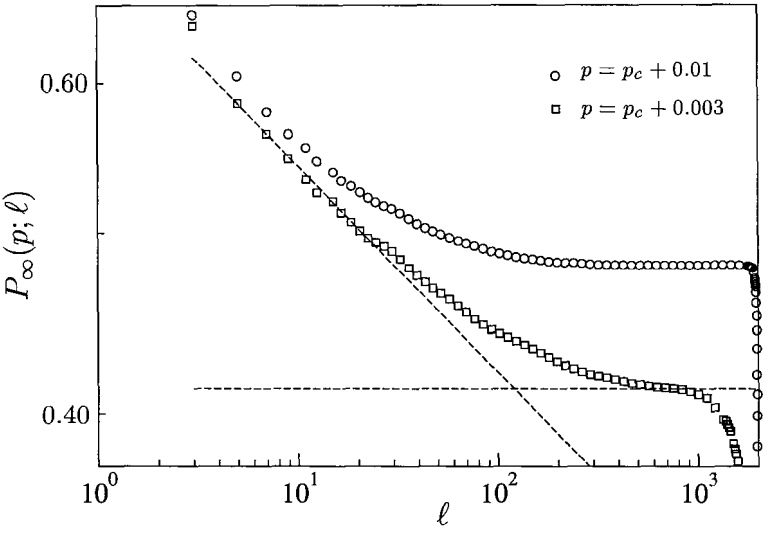

Fig. 1.33 Numerical results for the density of the percolating cluster, $P_\infty(p;\ell)$, versus the window size, ℓ, for two-dimensional site percolation on a square lattice of size $L = 5\,000$ at two different occupation probabilities $p > p_c$. Note that both axes are logarithmic. There is a crossover from fractal to uniform behaviour as ℓ increases.

1.8 Finite-Size Scaling

The problem of percolation is defined on an infinite lattice. In one dimension and on the Bethe lattice, exact results can be derived. For $d > 1$, we must resort to numerical results to verify theoretical predictions. Unfortunately, infinite lattices cannot be simulated. Fortunately, however, it is the size of the system relative to the correlation length that is important, rather than the absolute size of the system itself.